Observations of microphysics pertaining to the development of drizzle in warm, shallow cumulus clouds

Jeffrey R. French*, Gabor Vali, and Robert D. Kelly

University of Wyoming,
Laramie, WY, USA

*Corresponding Author: NOAA/ARL Field Research Division, 1750 Foote Dr., Idaho Falls, ID 83402, USA. fax: (208) 526-2549. email: jeff.french@noaa.gov

SUMMARY

The evolution of drizzle was studied in small cumulus clouds in a subtropical environment. Observations were made using three instrumented aircraft, a ground-based radar, and a 95 GHz airborne Doppler radar during the Small Cumulus Microphysics Study in east central Florida, summer 1995. Data from six clouds, from two days, are examined in this paper. Both sets of clouds were less than 2 km in depth at observation times; in-cloud temperatures were >10° C.

Droplet spectra observed in these clouds were generally bi-modal. The sizes of the droplets within the large mode are consistent with growth through condensation. It remains unclear how droplets within the small mode formed but their existence appears to be tied to entrainment and mixing.

Drizzle drops (drops with diameters >50 μm) were found at all levels in the clouds. The penetration-averaged concentrations of drizzle drops were less than 15 L^{-1}, except in the uppermost regions of clouds on one of the days where drizzle drop concentrations exceeded 100 L^{-1}. In general, the presence of drizzle drops in the upper regions of the clouds is consistent with models of droplet growth through condensation and stochastic collection. The existence of drizzle at low and midlevels may be due to collection initiated by ultra-giant aerosols, or to the redistribution of drizzle drops from neighboring or earlier cloud elements.

KEYWORDS: cumulus microphysics entrainment drizzle coalescence

1. INTRODUCTION

The *Glossary of Meteorology* defines a drizzle drop as "a drop of water of diameter 0.2 to 0.5 mm falling through the atmosphere." Further, all drops with diameters smaller than 200 μm are classified as cloud droplets. These definitions are well suited for an observer on the surface, but for studying droplet growth and the evolution of the droplet spectrum, it is more reasonable to use significantly smaller size limits for distinguishing between cloud droplets and drizzle drops. For this purpose, in the study presented here we define a drizzle drop as "any drop with a diameter greater than 50 μm" noting that in the study to be presented the concentration of such drops is less by several orders of magnitude than the concentration of the smaller cloud droplets. The development of drizzle drops in small cumuli is what is investigated.

How quickly drizzle develops depends to a large degree on the characteristics of the droplet spectra. Maritime cumuli having fewer but larger cloud droplets and droplet distributions with greater spectral widths are widely accepted as being able to produce drizzle more rapidly than their continental counterparts (Beard and Ochs 1993).

Two essential ingredients for efficient growth through collision/coalescence are large droplets (40 μm diameter is an oft-quoted size) and a broad size distribution. The development of large droplets may be explained by condensational growth given enough time. But, condensational growth alone leads to a narrow size distribution, quite different than the broader distributions observed in most maritime-type cumuli (*e.g.* Squires 1958, Warner 1969). Broadening toward smaller sizes may be accounted for through entrainment/mixing, although it is not clear exactly how such mixing occurs (Blyth 1993). Broadening toward larger sizes, on the other hand, is more difficult to explain.

It is misleading to consider that collision/coalescence plays no role in the early development of the droplet spectrum. As pointed out by Pruppacher and Klett (1997) and Jonas and Mason (1974), collision/coalescence is not a process that simply 'turns-on' once drops reach some critical size but rather is occurring at all times, gradually increasing in importance relative to condensation as droplet sizes increase. The key point for the broadening of droplet spectra is that even in the early stages, when the growth of the majority of droplets is dominated by condensation, a small fraction of the droplets become significantly larger by coalescence. These droplets then have increased probabilities for further growth by coalescence.

A major objective of the Small Cumulus Microphysics Study (SCMS) was to make detailed and coordinated measurements of the early development of large cloud droplets and the role of coalescence in warm cumuli. This paper contains results on the microphysical structure and evolution of these clouds from analysis of aircraft in situ measurements. In particular, the nature of the droplet spectrum and observations of drizzle drops are discussed. The observations are compared to model results of droplet growth presented by Flossman *et. al.* (1985). In addition, the relative contributions of cloud droplets and drizzle drops to the Rayleigh reflectivity factor are examined and shown to be roughly the same.

2. DATA SET

Conducted in east central Florida near the Kennedy Space Center (KSC) in summer 1995, SCMS utilized cloud radars and cloud penetrating aircraft to make observations of warm cumuli in their earliest stages. Three aircraft, the National Center for Atmospheric Research (NCAR) C-130, the University of Wyoming (UW) King Air, and the Meteo-France Merlin, made detailed measurements of clouds' microphysics. Two radars, the ground-based NCAR CP-2 and the Wyoming Cloud Radar (WCR) provided measurements of the Rayleigh scattering component of the reflectivity echo. In addition, CP-2 also provided an estimate of the Bragg scattering component at two wavelengths and the WCR provided high-resolution vertical cross sections of vertical Doppler velocity. A map of the study area over KSC including the location of the ground-based radar is shown in Fig. 1.

(a) Radar data

The CP-2 radar provided measurements of the back-scattered power at two wavelengths (3 and 10 cm). These measurements were used to determine both the Bragg and the Rayleigh components of the reflectivity through the method described by Knight and Miller (1998). For our analyses the CP-2 data were used to define general cloud characteristics such as cloud echo top height, maximum reflectivity and temporal evolution.

The WCR (3.2-mm wavelength) mounted on the King Air provided measurements of the Rayleigh reflectivity factor and the Doppler velocity at vertical incidence during each penetration. Because of the relatively short time required for a penetration, the WCR provided essentially instantaneous vertical cross-sections from the level of the King Air to cloud top. The high along-track resolution provided by this radar (roughly 10 m) allowed for direct comparisons of the radar data with in situ observations. Further information and results derived from this radar data set from SCMS are provided by French *et. al.* (1999).

(b) In situ data

Aircraft measurements from the C130, the Merlin, and the King Air are utilized in this paper. Data from the C130 and the Merlin used in this study have 1 Hz resolution. The King Air data has 30 Hz resolution for air motion and 10 Hz for microphysical parameters. Table 1 shows the specifications of the instruments used on the three aircraft for measurements of particle sizes and concentrations, vertical air motion, temperature, and cloud liquid water content.

All three aircraft were equipped with optical probes that provided measurements of the size and concentration of cloud particles with diameters from roughly 2 μm through several millimeters. Spectra for droplets with diameters of roughly 2 to 50 μm were determined from measurements made by PMS Forward Scattering Spectrometer Probes (FSSP) -100 (Dye and Baumgardner 1984). This probe yields concentrations for particles in 15 size channels with selectable size increments. Particle size spectra from FSSP-100 measurements cover from 2.7 to 54.8 μm for the Merlin, 2 to 30 μm for the King Air, and 5 to 47 μm for the C130.

An FSSP-300 mounted on the C130 detected particles with diameters between 0.3 and 20 μm; from this we use data for particles with diameters between 1 and 4 μm.

The data from the FSSP probes have been corrected for coincidence according to algorithms given by Brenguier (1989). No corrections are made for beam inhomogeneities (Baumgardner and Spowart 1990). Errors in droplet concentration are estimated to be 10 to

15%, based on total droplet concentrations of 300 to 600 cm^{-3} (Baumgardner *et. al.* 1985). Sizing errors are difficult to quantify; we estimate these to be roughly 10%, greater for higher concentrations (Cooper 1988).

Measurements of particles with diameters from 10 μm to a few hundred microns were made using PMS Optical Array Probes, OAPs (Knollenberg 1970). The King Air and the Merlin each carried a one-dimensional (OneDC) OAP-200X. This probe records counts in 15 size bins; from 12.5 to 187.5 μm on the King Air version and 20 to 300 μm on the Merlin version. The C130 carried an OAP-260X that operates on the same principle but records 64 channels corresponding to particle diameters from 10 to 640 μm. In regions of overlap between the FSSP and OneDC measurements, data from the FSSP were used. Thus the smallest size bins from OAP data used in this analysis are 37.5 μm for the King Air, 60 μm for the Merlin, and 50 μm for the C130

Each aircraft also carried OAPs to detect particles with diameters up to several millimeters, but for the clouds presented in this study, no drops larger than a few hundred microns were detected.

A thermal gradient diffusion chamber on the C130 provided measurements of cloud condensation nuclei (CCN; Hudson 1989). Low temporal resolution measurements of CCN concentrations for supersaturations between 0.01 and 1% were obtained.

The vertical air motion was determined by taking the difference between air relative and ground relative aircraft velocities. For all three aircraft, ground relative vertical aircraft velocities were determined from Inertial Reference Systems (IRS) and were corrected with pressure altitude in a baro-inertial loop. For vertical wind fluctuations with periods of less than roughly 60 s the IRS limits the accuracy of measurements, while measurements at lower frequencies are limited by the determination of static pressure. In general, the vertical velocity variations over roughly 60 s are accurate to within 0.1 m s^{-1} and are better for higher frequency. Determination of vertical air velocity for time scales greater than 60 s are accurate to within roughly 5% of the vertical speed of the aircraft. For conditions encountered in SCMS this is better than 1 m s^{-1}.

Rosemount probes (Stickney *et. al.* 1981) provided out-of-cloud measurements of temperature from all three aircraft. In-cloud measurements from the Merlin and King Air were from reverse-flow probes (Rodi and Spyers-Duran 1972). Comparisons reveal measurements from the three aircraft agree to within 1 °C. These measurements were then adjusted to account for differences in mean temperature from the different probes.

Three different instruments on the three aircraft provided measurements of cloud liquid water content (CLWC). Measurements on the Merlin were made with a CSIRO-King probe (King 1978); C130 measurements were provided by a Particulate Volume Monitor (PVM) 100A (Gerber *et. al.* 1994). Calculations of the third moment from the FSSP spectrum provided estimates of CLWC from the King Air. The CSIRO-King probe on the King Air was inoperative for the days examined here. Baumgardner (1983) reported uncertainties of 30 to 40% for CLWCs derived from FSSP measurements. With corrections for coincidence, we estimate the uncertainty of the King Air CLWC measurements at roughly 20%. Adding to our confidence, we find maximum CLWCs co-located with strong updrafts and generally within 5 to 10% of adiabatic values.

Comparisons from the FSSP probes and CSIRO-King probe from a flight for which all were mounted on the Merlin reveal that CLWCs from these instruments agree to within roughly 30% (Burnet 1999). In general, measurements from the Merlin and C130 FSSP probes were greater by 20 to 40% than measurements from the CSIRO-King and the King Air FSSP. Maximum CLWCs from the Merlin and C130 probes were greater than adiabatic values; while from the CSIRO-King and King Air probe they were less than adiabatic (Burnet 1999).

(c) Data coordination

The small size of the clouds observed in this study (diameters of roughly 1 km and cloud depths of 1.5 to 2 km) required careful coordination of aircraft and radar measurements. The movement and evolution of each cloud was tracked through the CP-2 data. Flight tracks based on Global Positioning Satellite (GPS) were used to associate the aircraft in situ data with radar echoes.

3. ENVIRONMENT CONDITIONS AND CLOUD CHARACTERISTICS

Soundings for the two study days here analyzed (5 August and 7 August) are shown in Fig. 2. These soundings were obtained from aircraft measurements before and after roughly 60-minute periods of cloud penetrations. There was no significant temporal evolution evident in these data, although nearby balloon soundings launched every few hours did reveal a slight strengthening and lowering of the inversion with time on 5 August.

The C130 provided observations of cloud base on 5 August and the King Air provided observations on 7 August. Cloud base conditions on these days were nearly identical, 910 mb (roughly 900 m MSL) and 21 °C. On both days, the mean lapse rate from the surface to cloud base was 6.5 °C km^{-1}. Subsidence inversions were located near 2 km on 5 August and at 1.5 km on 7 August. Observed cloud tops extended up to 1 km above these levels in spite of having very dry air throughout and above the inversions. The convective available potential energy (CAPE) calculated from the soundings was roughly 700 J kg^{-1} on 5 August and 300 J kg^{-1} on 7 August, indicating weak to moderate convection.

Winds from the surface to the inversion level were weak, less than 7 m s^{-1}. On 5 August the winds throughout this depth were easterly, while on 7 August, winds from the surface to cloud base were westerly, switching to a more easterly component above cloud base. Shear from cloud base to 2.5 km was weak, on the order of 10^{-3} s^{-1}.

Initial cloud formation on each day appeared to occur along a convergence boundary set up by a sea breeze front. The sea breeze front generally established itself early to mid-day and propagated inland as the day progressed. Initiation of convection was focused along this boundary. Clouds moved with the environmental wind at mid-levels.

Observations presented herein were made in small, relatively weak clouds such as shown in Fig. 3. Maximum measured Rayleigh reflectivity factors were less than 0 dBZ on 5 August and less than -5 dBZ on 7 August. Only one of the clouds, on 5 August, was observed to produce drizzle out of its base. The radar data reveal reflectivity echoes of roughly -15 dBZ extending downward from the base and observations of drizzle were noted in voice recordings of flight scientists on both the King Air and the C130.

(a) 5 August

The clouds on 5 August formed 15 to 20 km southeast of the CP-2 site, between the 135° and 140° azimuths. New clouds appeared continually in roughly the same area over a period of 45 minutes. Their movement was northwesterly, 4 to 6 m s^{-1}. The repetitive formation and movement resulted in 3 to 6 clouds existing at any one time along a northwest to southeast line. Clouds at the southeast end of the line were in their earliest stages of development while those at the northwest end were nearing the end of their life cycle. Typical cloud lifetimes were 30 minutes.

Aircraft penetrations were made along the cloud line, roughly through the center of each cloud, and reversing course at the end of the line. Repeated penetrations of the same cloud were separated in time by 3 to 7 minutes, depending on where along the line a particular cloud was located. The C130 made penetrations at 1.2-km altitude, the King Air at 1.6 km, and the Merlin at 2.5 km.

Although measurements were made in numerous clouds, the present analysis focuses on measurements made in three clouds designated as C5, C8, and C9. These clouds were selected on the basis of the availability of radar measurements throughout their lifetimes, the number of penetrations made through the clouds' center, and having in situ observations from more than one altitude.

Table 2 lists the general characteristics of these clouds. Cloud tops on 5 August varied between 2.0 and 2.9 km, depending on the stage of growth of the cloud. Maximum observed upward vertical velocities (from aircraft observations and the WCR) were between 5 and 7 m s^{-1}. The majority of the vertical velocity observations were in the range -2 m s^{-1} (downward) to +4 m s^{-1} (upward). [1]

Cloud liquid water contents as large as 2 g m^{-3} were observed in these clouds. At the flight level of the C130 (near cloud base) and of the UW King Air (700 m above cloud base) the largest values of observed CLWC were within 5% of adiabatic values. Near cloud top, maximum CLWCs from the Merlin were about 55% of the adiabatic values. At all levels, the largest CLWCs were co-located with the strongest updrafts.

Maximum observed droplet concentrations were 350 cm^{-3} at cloud base and at mid-levels. They were only slightly less, roughly 300 cm^{-3}, near cloud top. In general, regions of maximum droplet concentrations were co-located with the highest CLWCs and peak updrafts.

In-cloud temperatures were roughly 1 to 1.5° C colder than those expected from the soundings. Also, the temperature traces showed decreases in temperature upon entering cloud. At mid-levels, temperatures in regions of the highest cloud liquid water contents were roughly the same as the out-of-cloud temperatures. This indicates that the clouds were to a large degree negatively buoyant or the in-cloud measurements were in error.

(b) 7 August

The clouds on 7 August were more isolated than those observed on 5 August. The clouds formed in the southeastern quadrant of the CP-2 scan area, 15 to 25 km from the

[1] Hereafter, we will use the positive sign to designate upward moving air.

radar. Movement was westerly at less than 4 m s^{-1}. Again, typical radar observed lifetimes were on the order of 30 minutes.

Unlike on 5 August, the more isolated nature of the clouds allowed aircraft penetrations to be focused on a particular cloud. In general, 4 to 8 penetrations were made in any given cloud. Subsequent penetrations were separated in time by 2 to 4 minutes. Data are presented from three clouds on this day: C1, C4, and C10. The King Air made penetrations at mid-levels, from 1.3 to 2.2 km, with the majority made at around 1.6 km. The Merlin made penetrations between 1.6 and 1.9 km in C1. None of the study clouds were penetrated by the C130, although it did provide observations of CCN spectra near cloud base.

The general characteristics of clouds observed on 7 August (Table 2) were similar to those from 5 August. On this day cloud tops extended to 2.8 km, as much as 1.5 km above the base of the inversion. Peak vertical velocities were slightly stronger, 6 to 9 m s^{-1}. It is not clear from buoyancy considerations why vertical velocities were stronger on this day, but westerly winds in the sub-cloud layer may have resulted in stronger convergence along the sea breeze front.

At low levels, maximum observed CLWCs were nearly adiabatic. At mid-levels maximum CLWCs were roughly 60 to 90% adiabatic. At upper-levels maximum CLWCs were between 50 and 70% adiabatic. In general, at low altitudes there were more extensive regions with measured CLWCs within about 20% of adiabatic. As was the case with clouds on 5 August, the largest CLWCs were co-located with the strongest updrafts.

Cloud droplet concentrations on 7 August were greater than those observed on 5 August by about a factor of 2.5. At 1.2 km, maximum concentrations were 870 cm^{-3}; at 1.6 km, 850 cm^{-3}. Higher droplet concentrations on this day were probably due to westerly winds below cloud base associated with a more continental type CCN. Measurements made by the DRI CCN spectrometer below cloud base indicated that CCN concentrations at 1% supersaturation were larger by a factor of 2 than those observed on 5 August. The increased droplet concentrations had, predictably, some effect on the evolution of the droplet spectra and the development of drizzle drops in these clouds. These details are addressed in section 4.

(c) Vertical velocities and CLWC

Histograms of CLWC and of vertical velocities measured by the King Air in all penetrations are shown in Fig. 4. On both days, penetrations were made roughly 700 m above cloud base.

The distributions of liquid water contents and of vertical velocities are similar for the two days. Most of the cloud volumes had CLWCs between 0.5 and 1.5 g m^{-3}. Roughly 10% of the regions sampled on both days contained CLWC greater than 1.5 g m^{-3}. On both days, the adiabatic CLWC at this level was 1.95 g m^{-3}. On 5 August only 21% of the observations[2] were in regions where the CLWC was less than 0.5 g m^{-3}; 42% of the observations from 7 August were in such regions. The distributions of vertical velocities are quite symmetrical centered with modes of roughly 1 m s^{-1}. The distribution is wider for 7 August, yet values > 6 m s^{-1} comprise only 4% of the total.

[2] "Observation" used in this context refers to one 10 Hz sample.

4. CLOUD DROPLET OBSERVATIONS

(a) Fluctuations within penetrations

Figure 5 shows an example of traces of temperature, vertical velocity, droplet concentration, and CLWC for a penetration made by the King Air at 1.6 km (700 m above cloud base) on 5 August. Also shown are FSSP droplet spectra for selected regions indicated by arrows and labeled on the traces.

The traces of total droplet concentration and CLWC for this penetration are quite similar. The greatest CLWCs were encountered in regions A and F. These regions also contain the largest concentration of droplets. The correspondence between strong upward vertical velocities, positive temperature excursions, and regions of high CLWC and droplet concentration is also evident, though less precise. Regions with low CLWC generally correspond to reduced droplet concentrations, weak or downward moving air, and lower temperatures (regions C and G, for example). From King Air measurements during 13 penetrations on 5 August, correlation coefficients are 0.51 for vertical velocity and total droplet concentration, 0.87 for CLWC and total droplet concentration, 0.45 for temperature and total droplet concentration, and 0.57 for temperature and CLWC.

With the exception of regions with very low CLWCs and reduced droplet concentrations, where the droplet spectra are relatively flat (regions C and G), droplet spectra are bi-modal. One mode occurs at small diameters, less than 10 μm, and another at larger diameters, 20 to 40 μm, dependent on altitude. The small diameter mode tends to remain constant throughout penetrations; it is < 10 μm independent of altitude. The small mode is more pronounced at low and mid-levels. The size of the large diameter mode also remains constant within a cloud penetration but, unlike the small diameter mode, it has a strong dependence on altitude as also reported by Kitchen and Caughey (1981), Paluch and Knight (1984) and Paluch (1986). At diameters just a few microns larger than the large diameter mode, a very sharp decrease in the droplet concentration is always present in our observations.

For entire penetrations, the correlation between vertical velocities, CLWC, and droplet concentration are quite strong. Yet, there exist localized regions of about 100 m scale for which CLWC and droplet concentration are not well correlated. For example, region A (Fig 5) contains vertical velocities of roughly 4 m s^{-1} and CLWCs of nearly 2 g m^{-3}, while region B is located in an area of weak vertical motion and CLWCs of about 1.2 g m^{-3}. Yet, in both regions total droplet concentrations are roughly the same, 300 cm^{-3}. Spectra from these two regions reveal that in region A, nearly all of the droplets are clustered around the large diameter mode centered at 26 μm. In region B there are fewer droplets in the large mode and more droplets in the small mode.

In general, regions of reduced CLWC are associated with reductions in the concentration of droplets in the large mode with no shift of the mode to smaller sizes. This pattern can be further demonstrated by examining the relationships between the number concentration and volume mean diameter with the CLWC. Figure 6 shows scatter diagrams of the concentration of droplets within the large-size mode (20 to 30 μm for 5 August, 12 to 22 μm for 7 August) versus percent of adiabatic CLWC. Data in these plots were sampled at

10 Hz by the King Air and restricted to points where CLWCs were greater than 0.02 g m^{-3}. Correlation coefficients are between 0.84 and 0.92. There is a strong linear trend passing near the zero-zero point. Such would only be expected if the reduction of liquid water resulted from a reduced concentration of droplets in the large mode rather than a shift of the mode to smaller sizes. Figure 7 shows that the mean volume diameter varies only slightly and is nearly independent of CLWC.

In contrast, there is no correlation between the concentration of small cloud droplets (diameters 2 to 12 μm) and CLWC raising questions as to their origins. It is possible that the smaller droplets result from the partial evaporation of larger ones. Fig. 5e does reveal regions where some of the larger droplets appear to have evaporated to smaller sizes (regions D, E, and F) although such observations are more the exception rather than the rule. A more likely scenario is that smaller droplets are the result of the activation of new droplets in regions of reduced CLWC. However, there is only a weak positive correlation between the concentration of droplets in the small mode and the vertical velocity. Correlation coefficients for any given cloud are no larger than 0.35. On a broader basis, the average vertical velocity was greater for regions where the concentration of small droplets exceeded 25% of the total concentration compared to all regions in-cloud (1.4 m s^{-1} compared to 1.1 m s^{-1}). This suggests that re-activation may play a role but the results are far from conclusive.

(b) Averaged droplet spectra

Some features of the droplet spectra are best illustrated by data averaged for individual cloud passes. Such spectra are shown in Fig. 8 for three different altitudes for each study day.

The spectra in Fig. 8 indicate that both modes were discernible in the lower halves of the clouds, but the smaller mode became increasingly less distinct with increasing altitude. At mid-levels and below, droplets were often distributed roughly equally between the two modes. In the upper portion of cloud, the smaller mode was less pronounced. Also, the total droplet concentration remained nearly constant with altitude.

For a given day, the large diameter mode shifted to larger sizes with increasing altitude. The smaller mode, on the other hand, occurred at diameters between 2 and 6 μm independent of altitude. The diameters at which the two modes occurred remained nearly constant for various clouds sampled on a given day.

Comparing data from the two days, the larger mode occurred at a larger size when the total droplet concentration was less (5 August). The smaller mode, on the other hand, remained at nearly the same diameter.

A common feature found in all of the droplet spectra examined was a sharp decrease in droplet concentration at sizes just slightly larger than the second mode. Differential droplet concentrations decreased 2 to 3 orders of magnitude over a diameter interval of roughly 10 μm. To emphasize this pattern, we define a roll-off diameter designating the smallest size at which the slope of the log of the droplet concentration with respect to the diameter is less than -0.2. This corresponds to an average decrease in concentration of one order of magnitude over an interval of 5 μm in diameter. The dashed line in Fig. 8 indicates the roll-off diameter.

It seems reasonable that the roll-off diameter represents the maximum size achievable by droplets ascending from cloud base and growing through condensation. Thus, in considering condensation growth we utilize the roll-off diameter rather than the size of the large mode. Further, the roll-off diameter may be applied even for cases where a large droplet mode is either quite broad or ill-defined.

The observed roll-off diameters as a function of height above cloud base are shown in Fig. 9. The 5 August data are compiled from measurements from all three aircraft and comprise measurements made in 2 or 3 clouds at various stages of development. The 7 August data were obtained from measurements made by the King Air in three clouds at various altitudes and stages of growth.

On both days, the roll-off diameter increased with increasing height above cloud base. Compared to 7 August, the roll-off diameter on 5 August was slightly larger at all levels. This is consistent with the higher concentration of cloud droplets on 7 August.

5. OBSERVATIONS OF DRIZZLE DROPS

(a) Locations

The concentrations of drizzle drops (diameters > 50 μm) were 5 to 6 orders of magnitude less than the concentration of cloud droplets at the same level. In many instances the King Air detected only a few drizzle drops throughout entire penetrations. Because of this, estimates of local concentrations are essentially meaningless and it was necessary to average over entire penetrations to determine reasonable concentration estimates.

Examples of combined FSSP and OneDC droplet spectra are shown in Fig. 10. Note that in all cases the size distributions of drizzle drops are quite flat for diameters from roughly 70 to 200 μm.

For a given height above cloud base the concentration of drizzle drops was greater on 5 August than on 7 August. More rapid coalescence growth is to be expected for the 5 August clouds having larger cloud droplets.

The concentration of drizzle drops increased with increasing altitude. Between 300 and 500 m above cloud base, drizzle drops were detected in extremely low concentrations. Often only one or two droplets were detected through entire penetrations of roughly 1 km in length. This corresponds to an average concentration of roughly 0.2 L^{-1}. At mid-levels, drizzle drop concentrations were greater, generally a few per liter (5 to 50 droplets per penetration).

Concentrations of drizzle drops exceeding roughly 70 L^{-1} were only observed near cloud top on 5 August. At this level, the roll-off diameter had grown to sizes greater than 40 μm and concentrations of drops with diameters between 50 and 200 μm were as large as 250 L^{-1}.

The Merlin made 10 penetrations in three clouds near cloud top on 5 August from which 54 seconds of in-cloud data were collected. Thirty percent of those observations were within regions where drizzle drop concentrations were greater than 70 L^{-1} and 10% were within regions where drizzle concentrations were greater than 100 L^{-1}. There was little correlation between the concentration of drizzle and updraft velocity, but drizzle concentrations at this level were larger in regions with greater CLWCs. All of the

observations where drizzle concentrations were greater than 70 L^{-1} were in regions where the CLWC was greater than 1 g m^{-3}. The correlation coefficient between CLWC and drizzle drop concentration is 0.38.

Some comments can also be made regarding the CLWCs, vertical velocities, and radar reflectivity factors encountered at locations where drizzle drops were observed. Figure 11 shows a reflectivity image from the WCR and traces of CLWC and vertical velocity for the same penetration as shown in Fig. 5 (700 m above cloud base). The nearest usable range gate from the WCR was roughly 130 m above the flight level of the King Air, thus cloud edges deduced from the reflectivity images do not match perfectly with edges defined by CLWC measurements. The diamond symbols indicate locations where drizzle drops were detected at flight level. In general, drizzle drop observations were clustered in and around regions of high CLWC and radar reflectivity. Yet, not all of the drizzle was encountered in such regions. A number of drizzle drops were found near cloud edge or even completely outside of cloud. Such regions were devoid of cloud water and were normally associated with weak, downward motion.

Similar plots from penetrations in other clouds are shown in Figs. 12 and 13. For the penetration represented in Fig. 12, all of the drizzle drops detected by the King Air lie outside what appears in the radar image as the main region of the cloud. Drops detected between 0.1 and 0.2 km from the center of the cloud are associated with weak reflectivity and located within a region of low CLWC and downward vertical velocities. Drops detected between 0.3 and 0.6 km are found in moderate to strong upward motion, moderate CLWC, and relatively strong reflectivity factors (greater than -15 dBZ). These drops are probably associated with a region of new growth as it ascends through the flight level. The top of this bubble can be seen in the first few range gates in the reflectivity field.

On 7 August reflectivity factors were much lower (Fig. 13) than on 5 August. Drizzle drop locations from this penetration were sparsely spread throughout much of the cloud. But, there is some correspondence between echo strength and drizzle location with drizzle drops detected predominantly in regions of higher than average reflectivity.

The three examples in Figs. 11 through 13 illustrate the high degree of variability in the location of drizzle drops in the studied clouds.

(b) Statistics

On 5 August, drizzle drops were detected in only 13% of the observations made in-cloud 700 m above cloud base. Thirty-five percent of the drizzle drops were in regions with CLWC < 0.1 g m^{-3}. These observations correspond to regions of weak, downward moving air generally and were located near the edges or completely outside of clouds. For the remainder of this discussion, we focus on drizzle contained within regions with CLWC > 0.1 g m^{-3}.

Table 3 differentiates the frequency of observations with high CLWC and moderate to strong vertical velocities. Of the total 144 drops detected, 57% were in regions with CLWC > 1 g m^{-3}. This frequency is only slightly higher than the 50% for all observations with CLWC > 1 g m^{-3}.

Drizzle drops also tend to be contained within regions of moderate updraft. Nearly 29% of the drizzle drop observations on 5 August were in regions where the updraft was greater than 2.5 m s^{-1}, compared to only 19% of the total observations.

Data from 7 August reveal similar statistics, although observations of drizzle drops were significantly more rare. Only 3% of the total cloud regions sampled at mid-levels contained observations of drizzle drops. On 7 August a total of 21 drizzle drops were detected, of which only 2 were in regions where the CLWC less than 0.1 g m^{-3}. Again, there was a slight tendency for drizzle drops to occur in regions of moderate CLWC and upward air velocity. Thirty-two percent of the drizzle drops on this day were in regions where the CLWC was greater 1 g m^{-3}, 27% of the total observations were made in such regions. Also, 47% of the drizzle drops were located in updrafts of 2.5 m s^{-1} and greater, compared to only 41% of the total observations.

At mid-levels and above, drizzle drops were detected in every penetration. In general there was no trend between the amount of drizzle encountered and whether the penetration occurred early or late in the evolution of a cloud. Data from two of the clouds on 5 August did reveal an increase in drizzle concentration by roughly a factor of 1.5 from the first to last penetrations (at 700 m above cloud base). Data from other clouds, however reveal either no change or a pulsation in drizzle concentration over the lifetime of the cloud.

6. REFLECTIVITY CALCULATIONS

Since the Rayleigh reflectivity factor depends on the sixth moment of the size distribution it is often assumed that it is dominated by the larger particles. But, for size distributions with very steep slopes such as those observed on 5 August and 7 August, the contribution of smaller drops can be significant.

Reflectivity-weighted differential size distributions are shown in Fig. 14. The units of the ordinate in Fig. 14 are reflectivity per micron size interval. Integrating over all size ranges results in the total reflectivity, Z, in mm^6 m^{-3}. Calculations were based on FSSP and OAP OneDC data, assuming Rayleigh scatter.

In all cases, these distributions have two peaks, one at $d > 120$ μm and one that corresponds to the large droplet mode. The relative contributions from particles within the two size regimes to the total reflectivity were nearly constant throughout a given penetration, except in regions of downdrafts and low CLWCs. In those regions the reflectivity due to cloud droplets was negligible and drizzle drops dominated the total reflectivity.

Figure 15 shows the time evolution of the calculated reflectivity for four clouds. The reflectivity calculations are divided into that component due to cloud droplets (Z_C) and drizzle drops (Z_D) averaged over entire penetrations. In general Z_C and Z_D were always within a few dB of each other, independent of the level at which the observation was made. There was a slight tendency for Z_C to dominate the total reflectivity early and as time increased, Z_D would approach Z_C. The reflectivity due to drizzle drops, Z_D, in some instances increased throughout a cloud's lifetime and in other instances pulsated, first increasing then decreasing. At the same time, the reflectivity from cloud droplets, Z_C, remained relatively constant for a given level.

For a given level, Z_C was larger on 5 August than on 7 August. This is as expected since the roll-off diameter was larger on 5 August. At 700 m above cloud base Z_C was roughly -16 dBZ for clouds on 5 August and -21 dBZ for clouds on 7 August. At cloud top on 5 August, Z_C was roughly -10 dBZ. Also, Z_C varied by roughly 6 dB at any given level.

7. DISCUSSION

The microphysical character of the clouds from the two days differed significantly, although the environments in which the clouds evolved was quite similar. Key differences include: (1) higher cloud droplet concentrations on 7 August leading to (2) smaller cloud droplets eventually resulting in (3) fewer drizzle drops produced at a given level. Consequently, the clouds on 5 August were able to produce higher concentrations of drizzle drops, quicker and at lower altitudes, than the clouds on 7 August despite similarities in cloud top height, CLWC, and vertical velocity.

(a) Droplet growth by condensation

In order to provide a quantitative perspective for the observations described in the preceding sections we compare those observations with the calculations of Flossman *et. al.* (1985). Flossman *et. al.* (1985) modeled the evolution of droplet spectra using a single parcel model. Assuming an aerosol size distribution consistent with Dierdmendjian (1969) they calculated the evolution of the drop size distribution from activation through growth by condensation and collision/coalescence. Flossman *et. al.* used the numerical solution of Berry and Reinhardt (1974) to model coalescence growth from the stochastic collection equation.

The parcel model allows heat and mass transfer across the parcel boundaries to simulate entrainment. Lee and Pruppacher (1977) showed this parameterization to produce more realistic (broader) droplet spectra than its adiabatic (non-entraining) counter-part. Of course, such a model cannot treat effects due to settling and redistribution. Also, the single parcel description does not include complexities that arise from the interactions of multiple thermals which was shown to be the situation for the clouds here described (French *et. al.* 1999).

Results from two of the cases from Flossman *et. al.* were compared with our observations. Table 4 lists various parameters, including droplet concentration, cloud liquid water content, and vertical velocity for Cases 3 and 4 from the model and from observations in clouds on 5 August and 7 August. Case 3 from Flossman *et. al.* predicted droplet concentrations at 400 s into the simulation (roughly equivalent to 500 m above cloud base) of 700 cm^{-3}, compared to observed concentrations between 750 and 850 cm^{-3} for clouds on 7 August. CLWCs from the model were 0.33 g m^{-3} at 200 s and 0.77 g m^{-3} at 600 s. These values were lower (by roughly a factor of 3) than the maximum values observed on 7 August, but comparable with penetration-averaged values.

Case 4 from Flossman *et. al.* had lower predicted droplet concentrations than did case 3. At 400 s into the simulation, droplet concentrations were 360 cm^{-3}, compared to between 300 and 350 cm^{-3} for clouds on 5 August. Model predicted CLWCs were nearly identical with those from Case 3, and again lower than peak values. Penetration-averaged values were greater than model predicted values at low and mid-levels and less than model predicted values near cloud top.

In both model cases, the parcel was given an initial vertical velocity of 1 m s^{-1} at 900 mb, 20 °C and 90% relative humidity. From that point, vertical velocities increased to a maximum of roughly 2.5 m s^{-1} at about 800 s into the simulations, then decreased as the parcel continued to ascend. Peak values of vertical velocities on both days were considerably stronger, 6 to 8 m s^{-1}. However, French *et. al.* (1999) found that typical ascent rates for bubbles were between 1.5 and 2.5 m s^{-1} on 5 August and 1.5 and 4 m s^{-1} on 7 August. For purposes of comparison with a parcel model, the ascent rate of individual bubbles may be more appropriate than are peak vertical velocities.

Figure 16 shows mass-weighted droplet spectra at selected times from the model runs described by Flossman *et. al.*, and observed spectra from clouds on 5 August and 7 August taken from regions of moderate to high CLWCs. In the middle and upper levels, locations of the modes from the observed and modeled spectra are in reasonable agreement. In particular, the maximum sizes of the droplets are roughly the same in both the model and the observations. Spectra at lower levels do not match well, as observed spectra tend to be broader with modes occurring at larger sizes than the modeled spectra. These differences are linked to lower droplet concentrations and greater CLWCs in the observations compared to the model values.

(b) Development of drizzle

Near cloud top on 5 August observed spectra match well with model results from Flossman *et. al.* at 1400 s into the simulation (Fig. 16c). Of particular interest to this study is that drizzle drops (diameters larger than 50 μm) were beginning to be produced at this time in Case 4 and their production is attributed to growth through coalescence. A tail extends to sizes as large as 400 μm in diameter in the modeled distribution. Likewise, observed spectra also exhibit a tail to larger sizes. Conversely, no drizzle was produced in model Case 3, principally because droplet sizes were smaller due to the larger droplet concentrations resulting in reduced growth rates through coalescence.

Neither of the simulations described above predicted the development of drizzle within a few hundred meters above cloud base. The observations do reveal, however, the presence of drizzle in relatively low concentrations at mid-levels in these clouds. The concentration of drizzle at these levels in some cases remained constant and in other cases increased throughout the lifetime of the cloud. The latter may be the result of settling, transport, and/or redistribution of drizzle formed at higher levels in-cloud. Relatively high concentrations of drizzle in downdrafts near cloud edges on 5 August suggest that such a process may be occurring.

Multiple growth pulses may also affect the presence of drizzle at mid-levels. As discussed in French *et. al.* (1999) these clouds grew as a collection of multiple bubbles, ascending through the remnants of earlier bubbles. Thus, if drizzle is produced near cloud top in an earlier bubble, it may be carried down as the pulse decays and eventually entrained into a subsequent bubble. This may then explain the relatively high concentration of drizzle illustrated in Fig. 12. If that portion of the cloud near 0.5 km is a new bubble just passing the level of the King Air at the time of the penetration, then the drizzle associated with that portion of the cloud may be “left over” from a previous, decaying pulse.

Still, there exist cases where drizzle was observed in initial penetrations at mid-levels, just as the cloud top passed the level of the penetration for the first time. This suggests that an altogether different process may also be active.

Another possible explanation for the development of drizzle at mid-levels in low concentrations is formation on ultra-giant aerosols (UGA; Ludlam 1951). Observations in cloud free air have shown the existence of giant aerosols with diameters greater than 20 μm and concentrations as large 100 m^{-3} to 1000 m^{-3} (Woodcock 1953). Measurements during SCMS reveal similar concentrations (Laird *et. al.* 1998) and also show both a size and concentration dependence based on wind direction stratification (Blyth *et. al.* 1998). Based on data from a number of different days during SCMS, measurements made within the boundary layer between 500 and 1000 m reveal aerosol particles with diameters larger than 20 μm in concentrations of a few per liter for cases when low-level winds were out of the east. Concentrations were slightly less for westerly winds. Also, UGAs were significantly larger when the wind was easterly. In these conditions, UGAs as large as 100 μm were observed. In contrast, with westerly winds, the largest UGAs were roughly 30 μm. At lower and middle levels, drizzle concentrations and the concentration of UGAs, observed at cloud base altitudes, were comparable. Note also that the concentration of UGAs was less by an order of magnitude than the concentration of drizzle drops observed near cloud top on 5 August.

At any rate, the modeling study of Flossman *et. al.* (1985) is not a useful tool in determining which, if any, of these processes may be responsible for the occurrence of drizzle at mid-levels. The initial aerosol distribution used by Flossman did not include UGAs and the parcel model is not able to adequately represent particle redistribution. Any further work should require modeling of these processes.

(c) Role of entrainment and mixing

Condensation and collision/coalescence alone cannot explain many of the observed features of the droplet spectra. We begin by summarizing the observations of cloud droplet spectra: (1), the majority of the spectra in the lower and middle levels were bi-modal, while in the upper levels the spectra were generally uni-modal (Fig. 8); (2), the concentration of large cloud droplets was highly correlated with the CLWC while the mean volume diameter remained nearly constant (even for reduced CLWCs; Figs. 6 and 7); (3), for a given height above cloud base the diameter of the droplets at the larger mode remained constant through penetrations and throughout the lifetime of the cloud; and (4), the droplet diameter of the smaller mode was normally between 2 and 10 μm, although the precise location is difficult to establish because of the uncertainty in measurements from the FSSP in the lowest channels.

The strong linear correlation between the concentration of large cloud droplets and CLWC and the constancy of the large droplet mode indicate that the principal effect of mixing events on the cloud droplet spectrum was to reduce the concentration of the large-mode droplets while leaving their size unchanged (Austin *et. al.* 1985, Hill and Choularton 1985, Paluch 1986). Such observations are consistent with models of inhomogeneous mixing (Baker and Latham 1979), mixing with near saturated, but droplet free air (entity-type entrainment mixing; Telford and Chai 1980), or mixing which has occurred at scales not able to be resolved by the FSSP such that the distance traveled by the probe during the time

required to take a discrete sample (roughly 10 m) contains regions of both under-saturated, droplet-free air and near adiabatic air.

In regions where mixing had occurred at low and mid-levels, droplet spectra were normally bi-modal. In the upper regions of cloud, where mixing was even more pronounced (decreased CLWC) spectra were generally uni-modal. The same hypotheses that are able to explain the constancy of the large droplet mode may also account for the occurrence of the small droplet mode. If mixing events occur such that some of the large cloud droplets evaporate to smaller sizes while others remain unaffected, the end result is a bi-modal spectrum. Another hypothesis that has been proposed to explain the occurrence of bi-modal spectra is mixing followed by re-activation (Paluch and Knight 1984). In the cases studied here, the occurrence of significant concentrations of small droplets was related to lower CLWCs and slightly higher and predominantly upward vertical velocities. After mixing occurs, the droplet concentration is reduced (*as discussed above*), thus reducing the total droplet surface area. If this parcel then experiences ascent, the reduced surface area will result in higher supersaturations and therefore activation of CCN. This may explain why mixed regions were more bi-modal near cloud base but generally uni-modal near cloud top.

8. CONCLUDING REMARKS

The structure and microphysics of small cumuli observed in Florida on two days were quite similar in most regards except for clear differences in the developent of drizzle. These differences are the consequence of different CCN concentrations for the two days. The clouds were observed using in situ instruments mounted on three cloud penetrating aircraft and with radars.

Penetration-averaged droplet spectra were in general bi-modal. A sharp decrease in droplet concentration (termed the roll-off diameter) was observed at diameters just beyond the large mode. The roll-off diameter was observed to remain constant through entire penetrations. Further, it remained constant for all penetrations in all clouds at a given height above cloud base on a given day. It increased with height above cloud base in a predictable fashion. Differences in the roll-off size for the two days were the result of differences in droplet concentration.

Our data on the part of the spectra near the large mode does not provide a test of specific hypotheses of how entrainment and mixing results in a reduction of droplets while not changing the size of the large mode. The presence of the small droplet mode at low and mid-levels in clouds may be attributed to mixing followed by re-activiation, but could also have resulted from transport into the sampled cloud volumes from parcels of quite different previous histories. The pulsating nature of growth of these clouds is consistent with this idea.

Drizzle drops were encountered, in varying concentrations in all cloud penetrations, but it is clear that different mechanisms must be assumed to have led to the presence of the drizzle in different cloud regions. The main difference in this regard arises from the presence or absence of cloud droplets of about 40 μm diameter. In the upper regions of clouds where cloud droplets had grown to sizes larger than 40 μm the formation of drizzle can be explained by condensation and stochastic collection. Model simulations reported in the

literature show that drizzle drops are being produced at appreciable rates once cloud droplets achieve diameters larger than roughly 40 μm. However, the low concentrations of larger cloud droplets, especially in the upper regions of the clouds on 7 August, and the locations where some of the drizzle droplets were found with respect to the location of updrafts and regions of high CLWC, are clearly in conflict with the requirements for drizzle growth by coalescence indicated in even an entraining parcel. It is unclear whether these drizzle drops were initiated by UGA or were transported into the sampled volumes from other regions of the cloud. Concentrations of UGA within the boundary layer were comparable to the concentrations of drizzle observed in mid-levels. Also, the concentrations of UGAs were less and their sizes were smaller on days when winds were out of the west, consistent with the reduced drizzle concentrations on 7 August at low and mid-levels, further enhancing the plausibility of the explanation based on UGA. On the other hand, the relatively high concentration of droplets near cloud edge downdrafts supports the notion that drizzle was being transported downward from above. This supposition is also supported by the fact that drizzle concentrations increased throughout the lifetime of a cloud, giving more opportunities for drizzle drops produced in earlier thermals to be entrained into later ones. This effect goes beyond the benefits later parcels derive in a multi-bubble sequence from the enhanced moisture content of the environment and from reduced entrainment impact, as suggested by Mason and Jonas (1974) and Roesner et al. (1990). Detailed analysis of how drizzle drops survive evaporating parcels and get transported into newer cloud elements is beyond the scope of this paper.

Acknowledgments

We would like to thank the various groups who participated in SCMS and provided us with their data. In particular, we thank Meteo-France for the Merlin data, NCAR for the C130 and CP-2 data, and James Hudson from DRI for data from the CCN spectrometer. We also thank those involved with the UW King Air flight facility for their hard work during SCMS. Finally, we would like to thank Dr. Charles Knight for his discussions relating to droplet growth and drizzle and for sharing his insight into processes of entrainment/mixing. This research was supported under NSF grants ATM-9319907 and ATM-9712859.

REFERENCES

Austin, P. H., M. B. Baker, A. M. Blyth, and J. B. Jensen, 1985: Small-scale variability in warm continental cumulus clouds. *J. Atmos. Sci.,* **42**, 1123-1138.

Baker, M. B., and J. Latham, 1979: The evolution of droplet spectra and the rate of production of embryonic raindrops in small cumulus clouds. *J. Atmos. Sci.,* **36**, 1612-1615.

Baumgardner, D. and M. Spowart, 1990: Evaluation of the forward scattering spectrometer probe. Part III: Time response and laser inhomogeneity limitations. *J. Atmos. Oceanic Technol.,* **7**, 666-672.

Baumgardner, D., 1983: An analysis and comparison of five water droplet measuring instruments. *J. Clim. Appl. Meteorol.,* **22**, 891-910.

Baumgardner, D., W. Strapp, and J. E. Dye, 1985: Evaluation of the forward scattering spectrometer probe. Part II: Corrections for coincidence and dead-time losses. *J. Atmos. Oceanic Technol.,* **2**, 626-632.

Beard, K. V., and H. T. Ochs, 1993: Warm-rain initiation: An overview of microphysical mechanisms. *J. Appl. Meteorol.,* **32**, 608-625.

Berry, E. X., and R. L. Reinhardt, 1974: An analysis of cloud drop growth by collection. Part I: Double distributions. *J. Atmos. Sci.,* **31**, 1814-1824.

Blyth, A. M., 1993: Entrainment in cumulus clouds. *J. Appl. Meteorol.,* **32**, 626-641.

Blyth, A. M., J. Zhou, and J. Latham, 1998: Influence of ultra-giant nuclei on cumulus clouds observed during the small cumulus microphysics study in Florida. *Preprints, Conf. on Cloud Physics,* Am. Meteorol. Soc., Everett, WA, 492-493.

Brenguier, J. L., 1989: Coincidence and dead-time corrections for particle counters. Part II: High concentration measurements with an FSSP. *J. Atmos. Oceanic Technol.,* **6**, 585-598.

Burnet, Frédéric, 1999: Validation des Mesures Aeroportees de la Microphysique Nuageuse et Etude des Processus D'Entrainement-melange dans les Nuages Convectifs. Ph. D. Thesis *Universite Paul Sabatier Toulouse III*.

Cooper, W. A., 1988: Effects of coincidence on measurements with a forward scattering spectrometer probe. *J. Atmos. Oceanic Technol.,* **5**, 823-832.

Deirmendjian, D., 1969: *Electromagnetic Scattering on Spherical Polydispersions.* American Elsevier, 290 pp.

Dye, J. E., and D. Baumgardner, 1984: Evaluation of the forward scattering spectrometer probe. Part I: Electronic and optical studies. *J. Atmos. Oceanic Technol.,* **1**, 329-344.

Flossman, A. I., W. D. Hall, and H. R. Pruppacher, 1985: A theoretical study of the wet removal of atmospheric pollutants. Part I: The redistribution of aerosol particles captured through nucleation and impaction scavenging by growing cloud drops. *J. Atmos. Sci.,* **42**, 582-606.

French, J. R., G. Vali, R. D. Kelly, 1999: Evolution of small cumulus clouds in Florida: Observations of pulsating growth. *Atmos. Res.,* **52**, 143-165.

Gerber, H., B. G. Arends, and A. S. Ackerman, 1994: New microphysics sensor for aircraft use. *Atmos. Res.*, **31**, 235-252.

Hill, T. A., and T. W. Choularton, 1985: An airborne study of the microphysical structure of cumulus clouds. *Q. J. R. Meteorol. Soc.*, **111**, 517-544.

Hudson, J. G., 1989: An instantaneous CCN spectrometer. *J. Atmos. Oceanic Technol.*, **6**, 1055-1065.

Jonas, P. R., and B. J. Mason, 1974: The evolution of droplet spectra by condensation and coalescence in cumulus clouds. *Q. J. R. Meteorol. Soc.*, **100**, 286-295.

King, W. D., D. A. Parkin, and R. J. Handsworth, 1978: A hot-wire liquid water device having fully calculable response characteristics. *J. Appl. Meteorol.*, **17**, 1809-1813.

Kitchen, M., and S. J. Caughey, 1981: Tethered-balloon observations of the structure of small cumulus clouds. *Q. J. R. Meteorol. Soc.*, **107**, 853-874.

Knight, C. A., and L. J. Miller, 1998: Early radar echoes from small, warm cumulus: Bragg and hydrometeor scattering. *J. Atmos. Sci.*, **55**, 2974-2992.

Knollenberg, R. G., 1970: The optical array probe: An alternative to scattering or extinction for airborne particle size determination. *J. Appl. Meteorol.*, **9**, 86-103.

Laird, N. F., H. T. Ochs, R. M. Rauber, L. J. Miller, 1998: Microphysical properties of Florida small cumulus clouds. Part I: Observations. *Preprints, Conf. on Cloud Physics*, Am. Meteorol. Soc., Everett, WA, 486- 489.

Lee, I. N., and H. R. Pruppacher, 1977: A comparative study on the growth of cloud drops by condensation using an air parcel model with and without entrainment. *Pure Appl. Geophys.*, **115**, 521-545.

Ludlam, F. H., 1951: The production of showers by the coalescence of cloud droplets. *Q. J. R. Meteorol. Soc.*, **77**, 402-417.

Mason, B. J., and P. R. Jonas, 1974: The evolution of droplet spectra and large droplets by condensation in cumulus clouds. *Q. J. R. Meteorol. Soc.*, **100**, 23-38.

Paluch I. R. and C. A. Knight, 1984: Mixing and the evolution of cloud droplet size spectra in a vigorous continental cumulus. *J. Atmos. Sci.*, **41**, 1801-1815.

Paluch, I. R., 1986: Mixing and the cloud droplet size spectrum: Generalizations from the CCOPE data. *J. Atmos. Sci.*, **43**, 1984-1993.

Pruppacher, H. R., and J. D. Klett, 1997: *Microphysics of Clouds and Precipitation.* 2nd revised and enlarged ed., Kluwer Academic Publishers, Dordrecht, Holland, 954 pp.

Rodi, A. R., and P. A. Spyers-Duran, 1972: Analysis of time response of airborne temperature sensors. *J. Appl. Meteorol.*, **11**, 554-556.

Roesner, S., A. I. Flossman, and H. R. Pruppacher, 1990: The effect on the evolution of the drop spectrum in clouds of the preconditioning of air by successive convective elements. *Q. J. R. Meteorol. Soc.*, **116**, 1389-1403.

Stickney, T. M., M. W. Shedlov, D. I. Thompson, and F. T. Yakes, 1981: Rosemount total temperature sensors. Rosemount Inc. Tech. Report 5755, 28 pp.

Squires, P., 1958: The microstructure and colloidal stability of warm clouds. *Tellus*, **10**, 256-271.

Telford, J. W., and S. K. Chai, 1980: A new aspect of condensation theory, *Pure Appl. Geophys.*, **118**, 720-742.

Warner, J., 1969: The microstructure of cumulus clouds. Part I: General features of the droplet spectrum. *J. Atmos. Sci.*, **26**, 1049-1059.

Woodcock, A. H., 1953: Salt nuclei in maritime air as a function of altitude and wind force. *J. Meteorol.*, **10**, 362-371.

TABLE 1. SUMMARY OF PARAMETERS AND MEASURING DEVICES USED IN THIS STUDY

Variable	Instrument	Aircraft	Range	Resolution / Response	Accuracy
CCN spectra	CCN spectrometer	C130	0.02 to 1.0% supersaturation	0.02 to 0.1% supersaturation	
Cloud particle spectra	FSSP-300	C130	0.3 to 20 µm	0.05 to 2.0 µm	*see text**
	FSSP-100	C130	2.0 to 47 µm	3.0 µm	*see text**
		King Air	2.0 to 30 µm	2.0 µm	*see text**
		Merlin	2.7 to 54.8 µm	3.72 µm	*see text**
	OAP-200X	King Air	12.5 to 187 µm	12.5 µm	*see text**
		Merlin	20 to 300 µm	20 µm	*see text**
	OAP-260X	C130	10 to 640 µm	10 µm	*see text**
Cloud liquid water	CSIRO-King	C130 Merlin	up to 3 g m^{-3}	5 to ~ 60 µm**	10 to 20%
	PVM-100A	C130	> 3 g m^{-3}	2 to 70 µm**	5 to 10%
	FSSP-calculated	King Air	> 3 g m^{-3}	2 to 30 µm**	~ 30%
Temperature	Rosemount	C130 King Air Merlin	-50 to 50 °C	0.01 °C	0.5 °C out of cloud
	Reverse-flow	King Air Merlin	-50 to 50 °C	0.01 °C	0.5 °C out of cloud
Vertical winds	*see text*	C130 King Air Merlin	unlimited		0.1 m s^{-1} high freq. 1 m s^{-1} low freq.
Horizontal location	Tremble GPS	C130 King Air Merlin	unlimited		*at least* 100 m
Vertical location	Radar altimeter	King Air Merlin	several km		better than 10 m
	INS corrected	C130	several km		~ 25 m

* There are a variety of factors which influence the accuracy of the PMS probes. Some of these factors are touched upon in the text and numerous references are given for those who wish to examine these issues more deeply.

** The liquid water probes respond to droplet diameters in the given size ranges.

TABLE 2. SUMMARY OF CLOUD CHARACTERISTICS

Day	Cloud	echo top (km)	number of Pens	Alt. (km)	Alt. wrt cld.base (m)	Vert. wind ($m\ s^{-1}$)	CLWC ($g\ m^{-3}$) (*max; % adiab.*)	N_C (cm^{-3}) (*max*)
5 Aug	C5	2.7	3; King Air	1.61	710	-4.0 to 6.0	1.95; 100%	310
			4; Merlin	2.55	1650	-2.8 to 4.9	1.7; 53%	300
	C8	2.6	4; C130	1.2	300	-1.2 to 3.6	0.9; 100%	310
			6; King Air	1.61	710	-2.4 to 4.5	2.1; 105%	330
			2; Merlin	2.6	1700	-2.4 to 2.5	1.7; 53%	300
	C9	2.9	4; C130	1.2	300	-2.0 to 4.1	0.9; 100%	350
			4; King Air	1.60	700	-2.9 to 4.5	1.7; 87%	280
			4; Merlin	2.55	1650	-4.1 to 6.1	1.8; 56%	300
7 Aug	C1	2.2	4; King Air	1.28	380	-2.5 to 4.4	1.2; 109%	700
			5; Merlin	1.6	700	-3.8 to 2.9	1.0; 52%	880
			3; Merlin	1.89	990	-2.2 to 2.2	1.15; 48%	600
	C4	2.4	1; King Air	1.27	370	-1.0 to 5.2	1.0; 91%	870
			2; King Air	1.57	670	-1.9 to 6.5	1.5; 88%	800
			1; King Air	1.95	1050	-4.7 to 1.8	1.6; 67%	550
	C10	2.8	5; King Air	1.62	720	-5.2 to 8.5	2.0; 100%	800
			1; King Air	1.95	1050	-3.6 to 8.1	2.4; 100%	800
			1; King Air	2.15	1250	-5.8 to 0.5	2.0; 71%	600

TABLE 3. KING AIR OBSERVATIONS MADE IN REGIONS OF HIGH CLWC AND STRONG, UPWARD VERTICAL VELOCITY

Day		number of observations	% total observations	% observations (CLWC > 1 g m^{-3})	% observations (w > 2.5 m s^{-1})
5 August	all	1698	100	50	19
	drizzle	144	8	57	29
7 August	all	560	100	27	41
	drizzle	19	3	32	47

"all" includes all 10 Hz observations made by the King Air on a given day, "drizzle" includes only those instances where drizzle was detected. For both, only regions with CLWCs greater than 0.1 g m^{-3} were included in this analysis (*see text*).

TABLE 4. COMPARISON BETWEEN OBSERVATIONS AND MODEL RESULTS

Day/Model Run	level* (m) obs.	alt.** (m) model	time (s) model	CLWC ($g\ m^{-3}$) obs.	CLWC ($g\ m^{-3}$) model	vert. velocity ($m\ s^{-1}$) obs.	vert. velocity ($m\ s^{-1}$) model	droplet conc. (cm^{-3}) obs.	droplet conc. (cm^{-3}) model
5 August/	250	200	200	0.9(0.7)	0.32	4.1(2.2)	1.3	350(300)	460
Case4	700	760	600	2.0(1.1)	0.76	4.9(2.6)	2.1	330(230)	342
	1700	2090	1400	1.7(0.8)	1.36	5.9(2.4)	1.9	300(190)	249
7 August/	300	200	200	1.1(0.6)	0.33	5.2(2.4)	1.3	870(720)	740
Case 3	700	760	600	2.0(0.7)	0.77	8.5(2.2)	2.1	880(690)	694
	1100	1260	1000	2.3(0.8)	1.09	8.0(2.1)	2.2	800(640)	660

* altitude above cloud base

** approximate altitude above cloud base for model

Model results are from Flossman *et. al.* (1985). For the observed values, both the maximum and penetration-averaged (in parentheses) values are given.

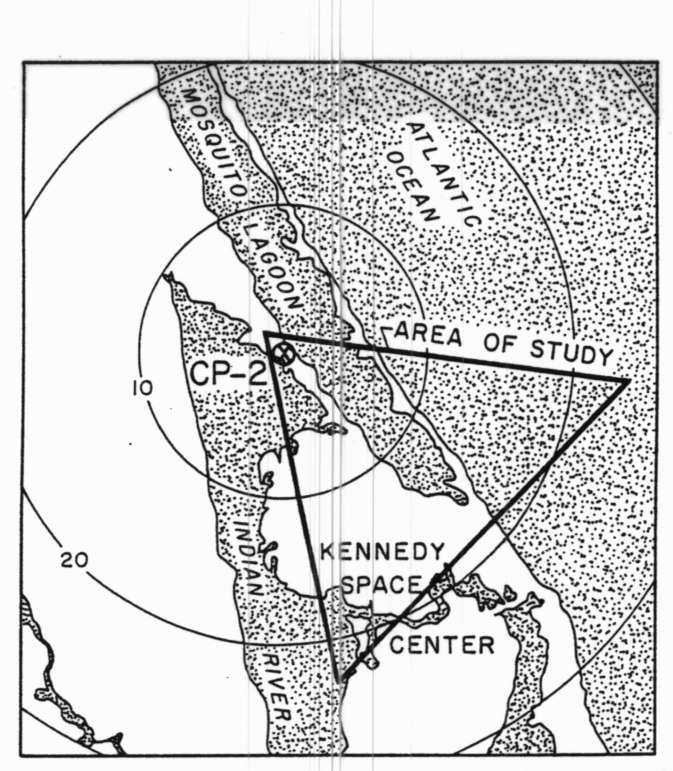

Fig. 1. Map showing the location of the CP-2 radar site and selected range rings (km). The triangle indicates the primary study area for SCMS.

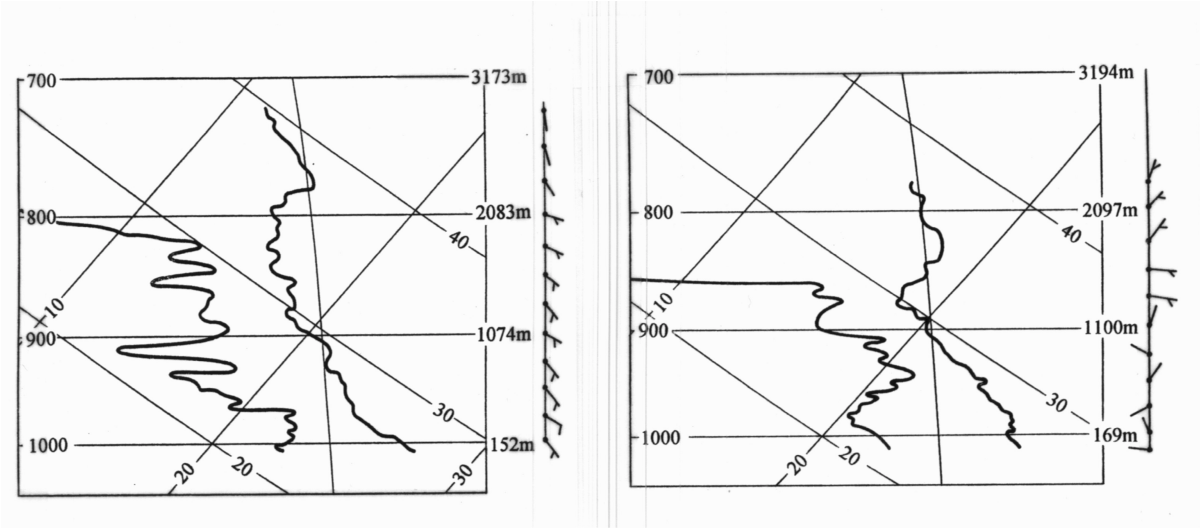

Fig. 2. Atmospheric soundings of temperature and dew point for (a) 5 August and (b) 7 August. These represent composite data compiled from aircraft measurements made both before and after a 1 hour period of cloud penetrations.

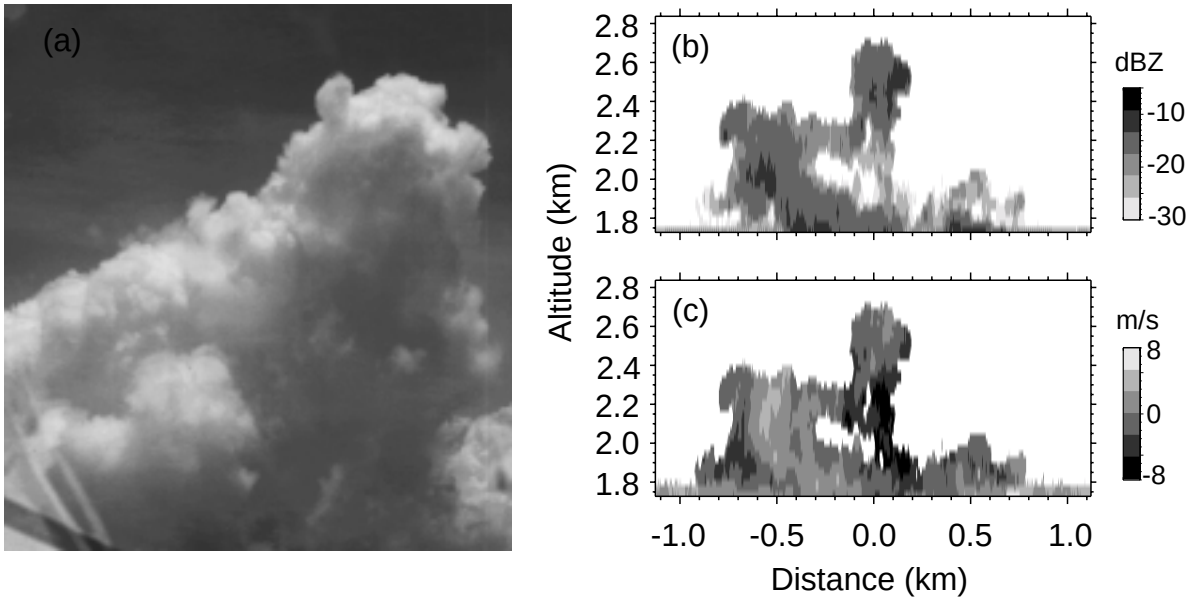

Fig. 3. A “typical” cloud observed during SCMS. On the left (a) is a picture of cloud C10 on 7 August taken from the King Air approximately 30 s before penetration. The images on the right are reflectivity (b) and vertical Doppler velocity (c) measured from the WCR during the penetration.

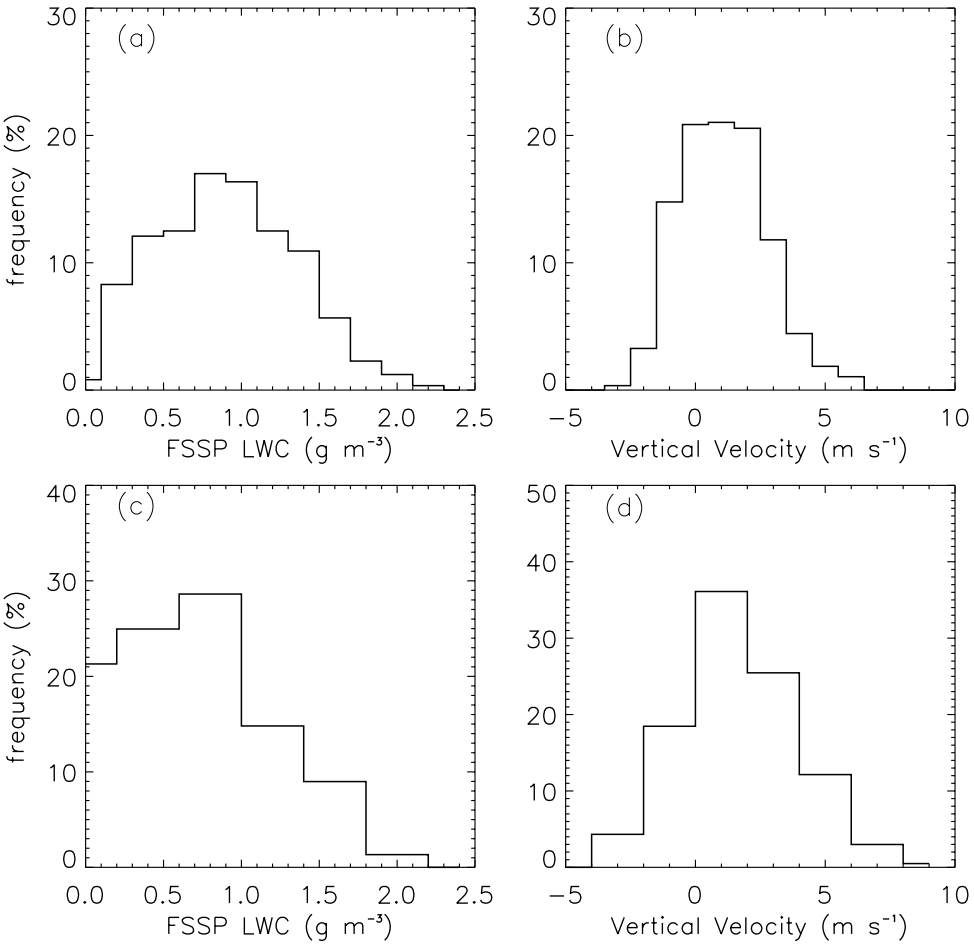

Fig. 4. Distributions of cloud liquid water content and vertical velocity compiled from (a & b) 13 penetrations in 3 clouds on 5 August and (c & d) 7 penetrations in 2 clouds on 7 August. All penetrations were made at roughly 600 m above cloud base. The adiabatic LWC was 1.95 g m^{-3}. Distributions were computed from all observations where CLWC was greater than 0.02 g m^{-3}. There were a total of 1712 observations on 5 August and 601 observations on 7 August.

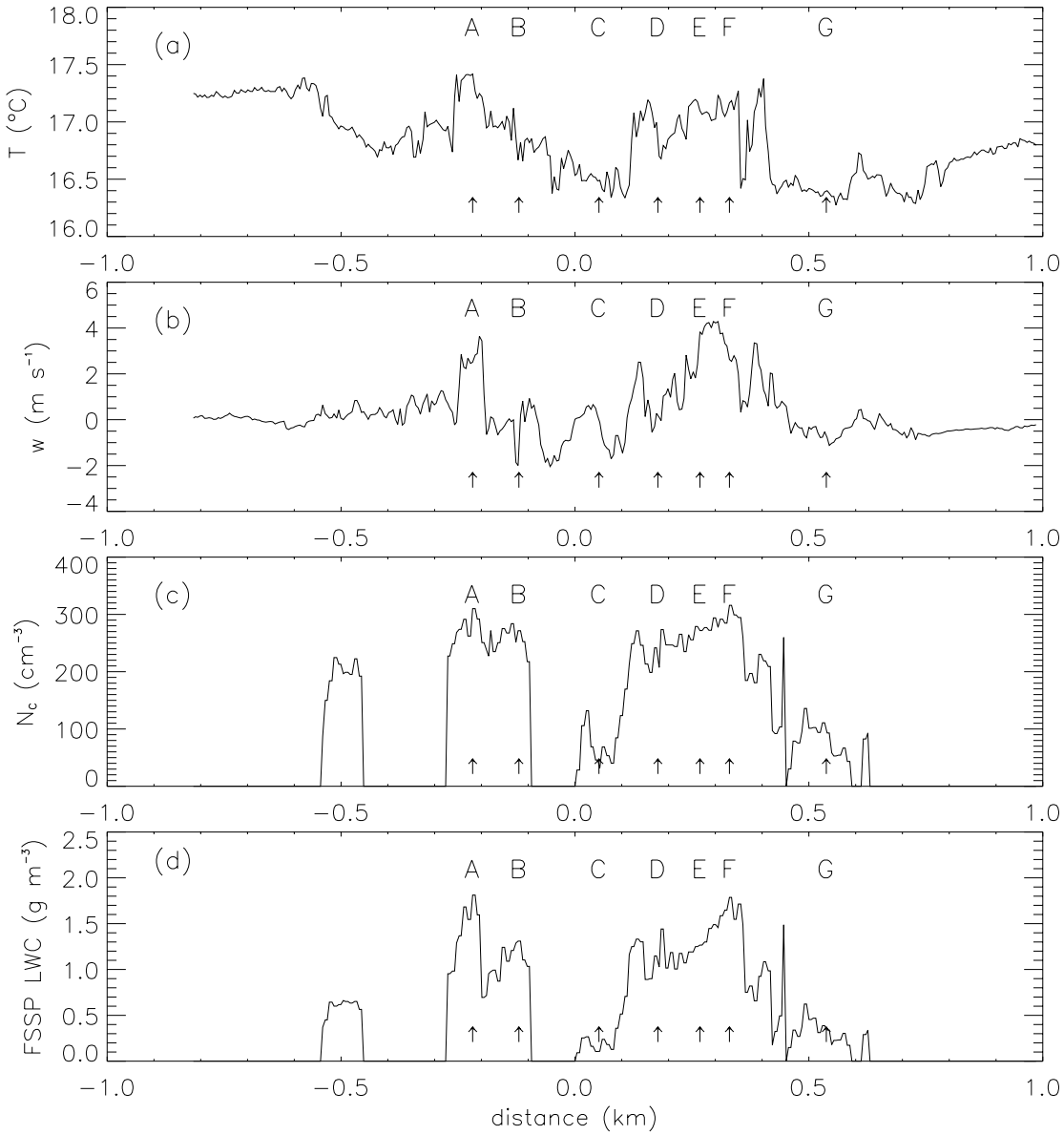

Fig. 5. Traces of (a) temperature, (b) vertical velocity, (c) total FSSP droplet concentration and (d) FSSP calculated liquid water content for the second penetration by the King Air of cloud C8 on 5 August. Droplet spectra (e) from seven regions labeled A through G are also shown.

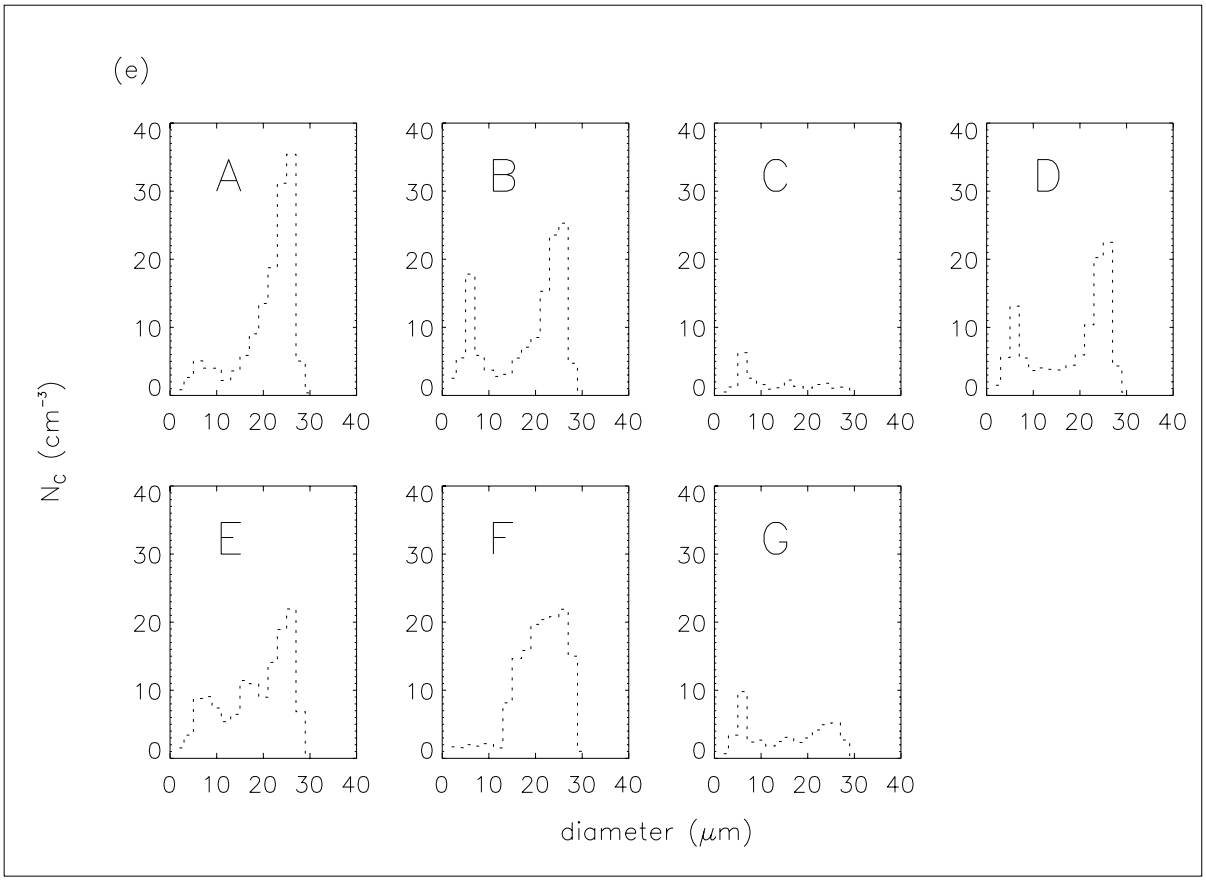

Fig. 5. *continued*

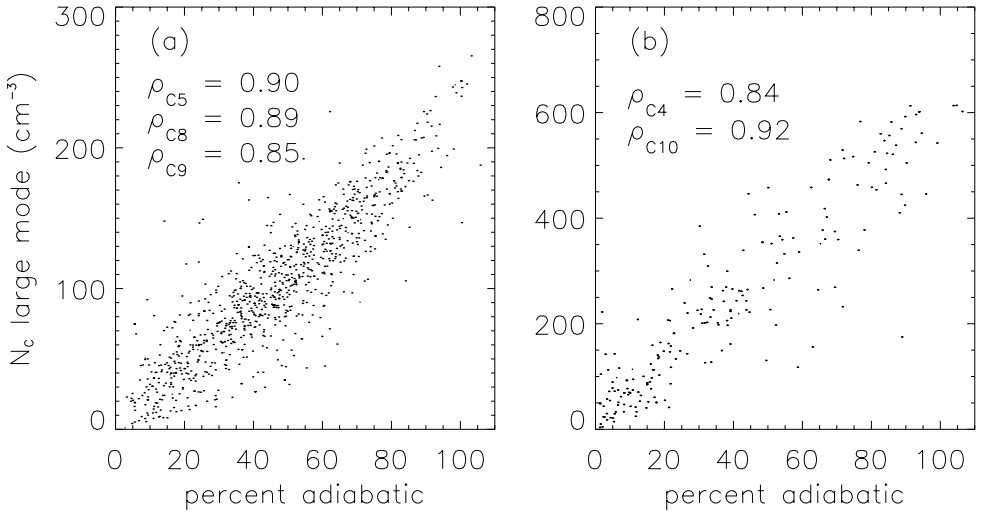

Fig. 6. Scatter plots showing the number concentration of cloud droplets within the large mode as a function of the percent of the adiabatic CLWC. These data were obtained by measurements made at roughly 600 m above cloud base by the King Air during (a) 12 penetrations of 3 clouds on 5 August and (b) 7 penetrations of 2 clouds on 7 August. For the clouds on 5 August the large mode was considered between 20 and 30 μm; on 7 August, between 12 and 22 μm. The value of ρ corresponds to the linear correlation coefficient calculated from data collected during all penetrations of a given cloud.

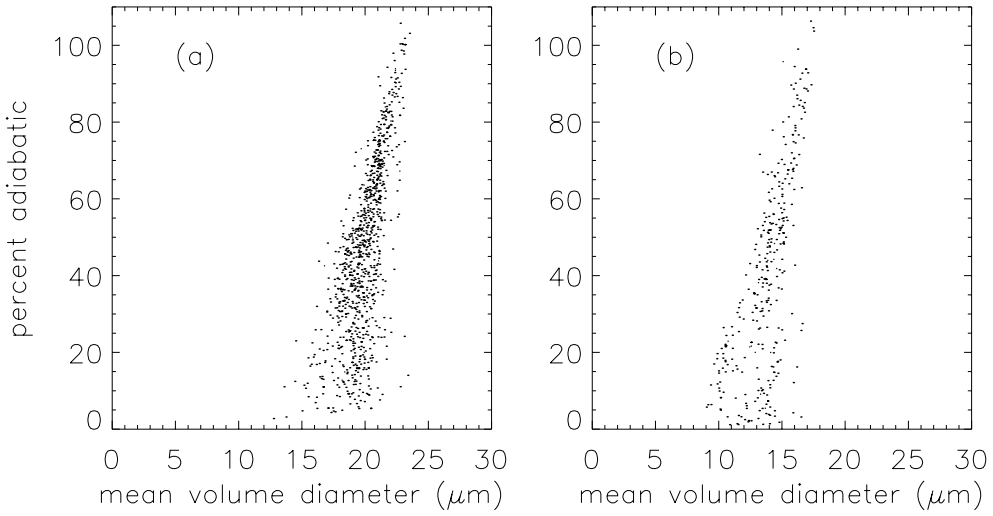

Fig. 7. As in Fig. 6, except for the mean volume diameter of the spectrum.

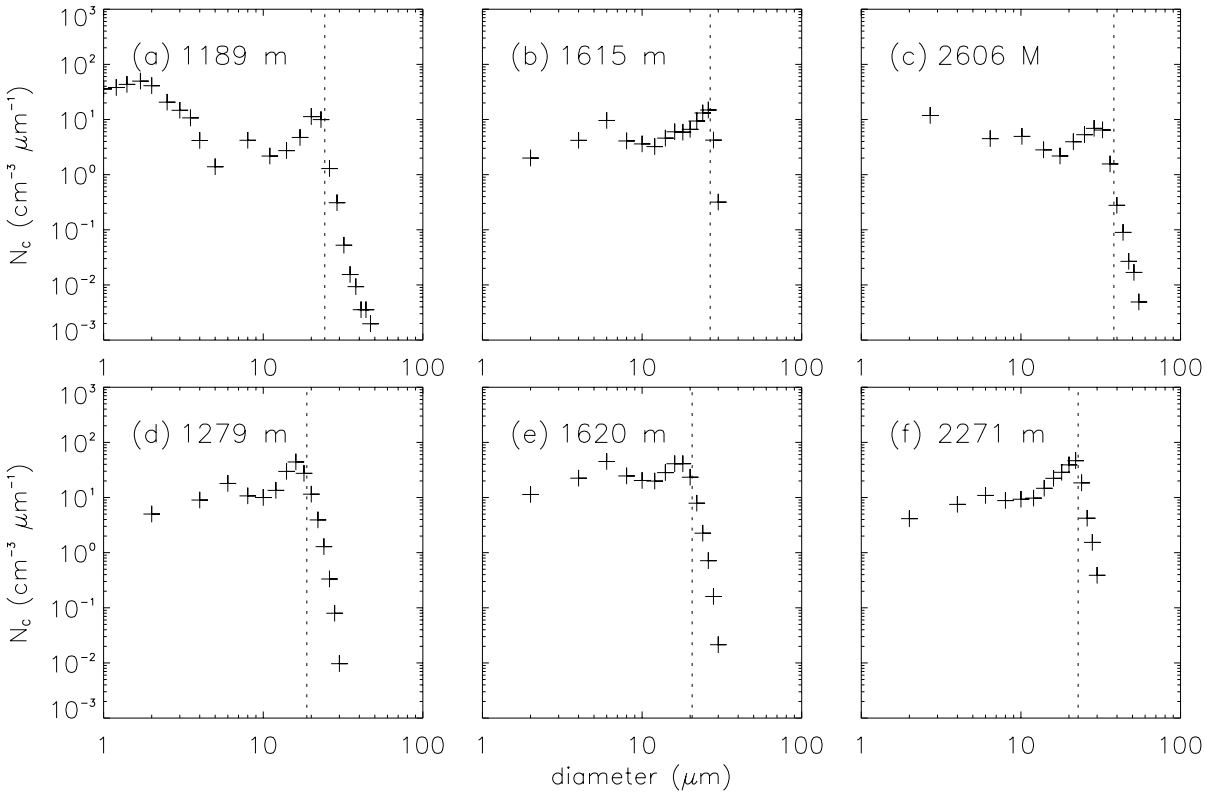

Fig. 8. Differential droplet concentration as a function of droplet diameter averaged over entire penetrations. The top three are from three penetrations on 5 August made in clouds (a) C9 by the C130 at 1.2 km, (b) C8 by the King Air at 1.6 km, and (c) C5 by the Merlin at 2.6 km. The bottom three are from three penetrations made by the King Air on 7 August; in clouds (d) C1 at 1.3 km, (e) C4 at 1.6 km, and (f) C10 at 2.3 km. The dotted line represents the roll-off diameter (*see text*).

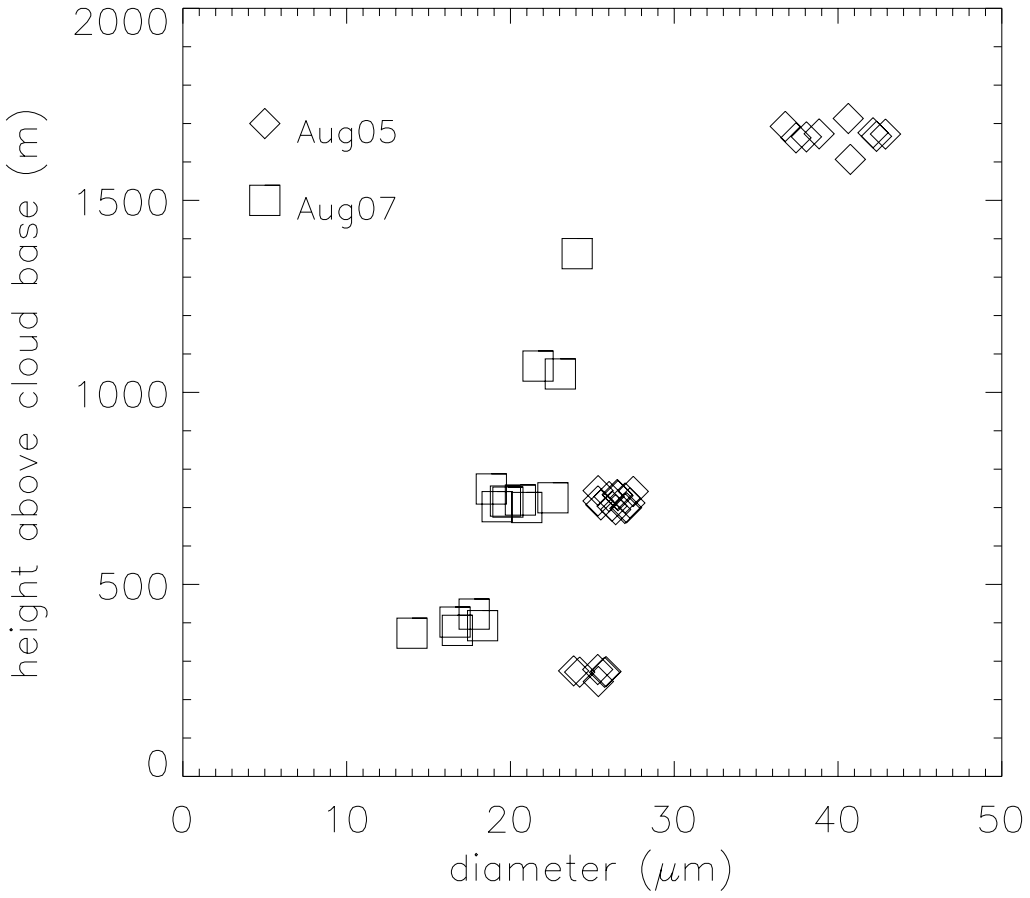

Fig. 9. The roll-off diameter as a function of height above cloud base for measurements made during 31 penetrations in clouds on 5 August and 15 penetrations in clouds on 7 August. In an effort to better depict overlapping points at a given level, symbols were shifted up to ±1.5 μm in diameter.

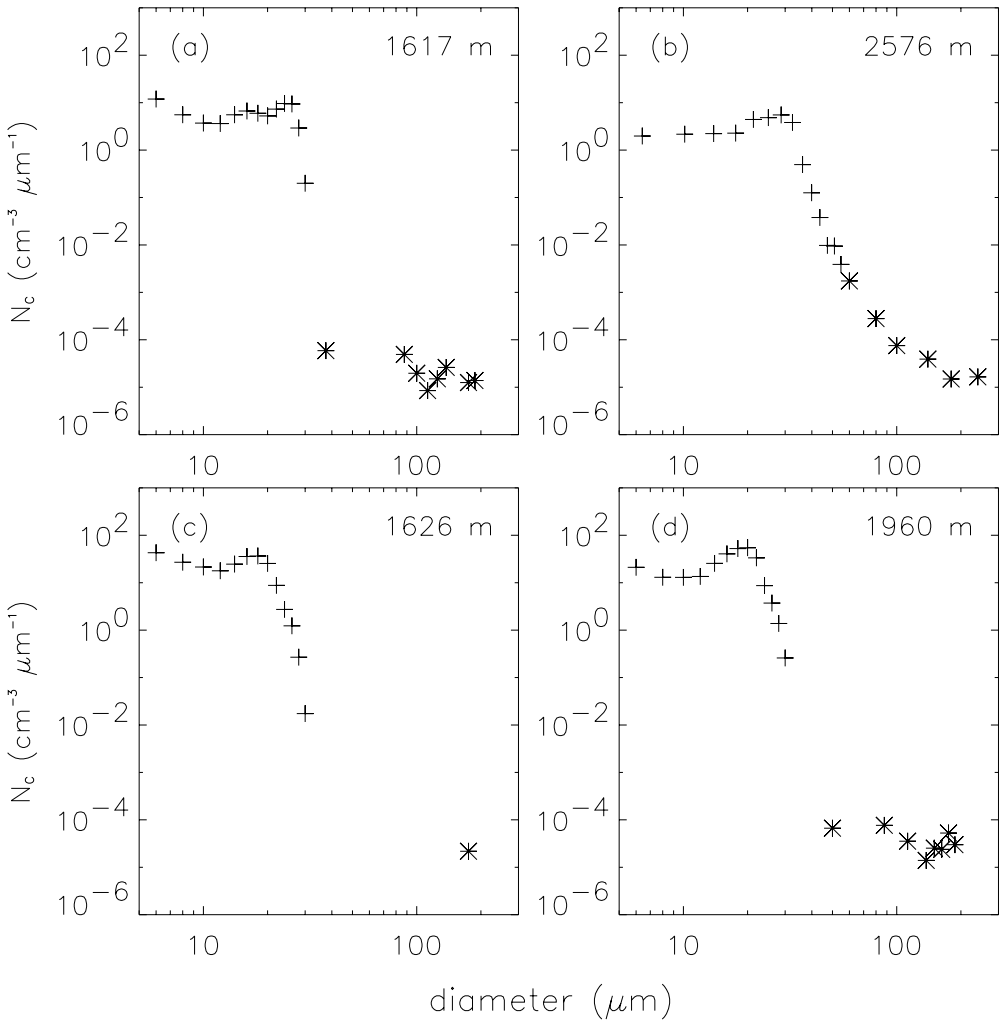

Fig. 10. Combined FSSP (+) and OneDC (*) spectra averaged over entire penetrations. Plots in the top row are from two penetrations of cloud C5 on 5 August at (a) 1.6 km by the King Air and (b) 2.6 km by the Merlin. Plots in the bottom row are from two penetrations of cloud C10 on 7 August by the King Air, made at (c) 1.6 km and (d) 2.0 km.

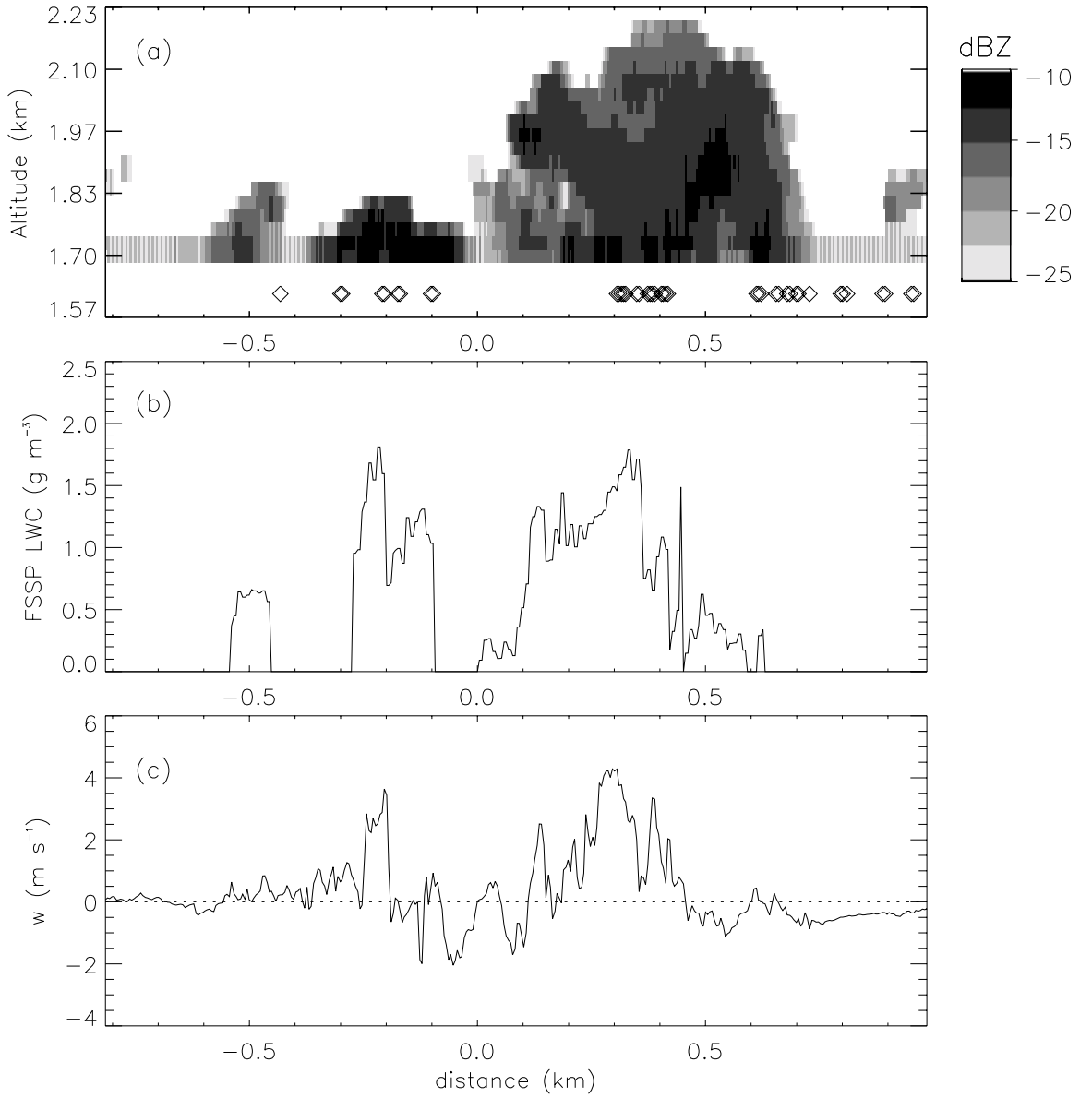

Fig. 11. (a) Vertical cross section of reflectivity from the WCR and traces of (b) CLWC and (c) vertical velocity for the second penetration by the King Air of cloud C8 on 5 August at 700 m above cloud base. Diamonds indicate locations where drizzle drops were detected by the OneDC probe.

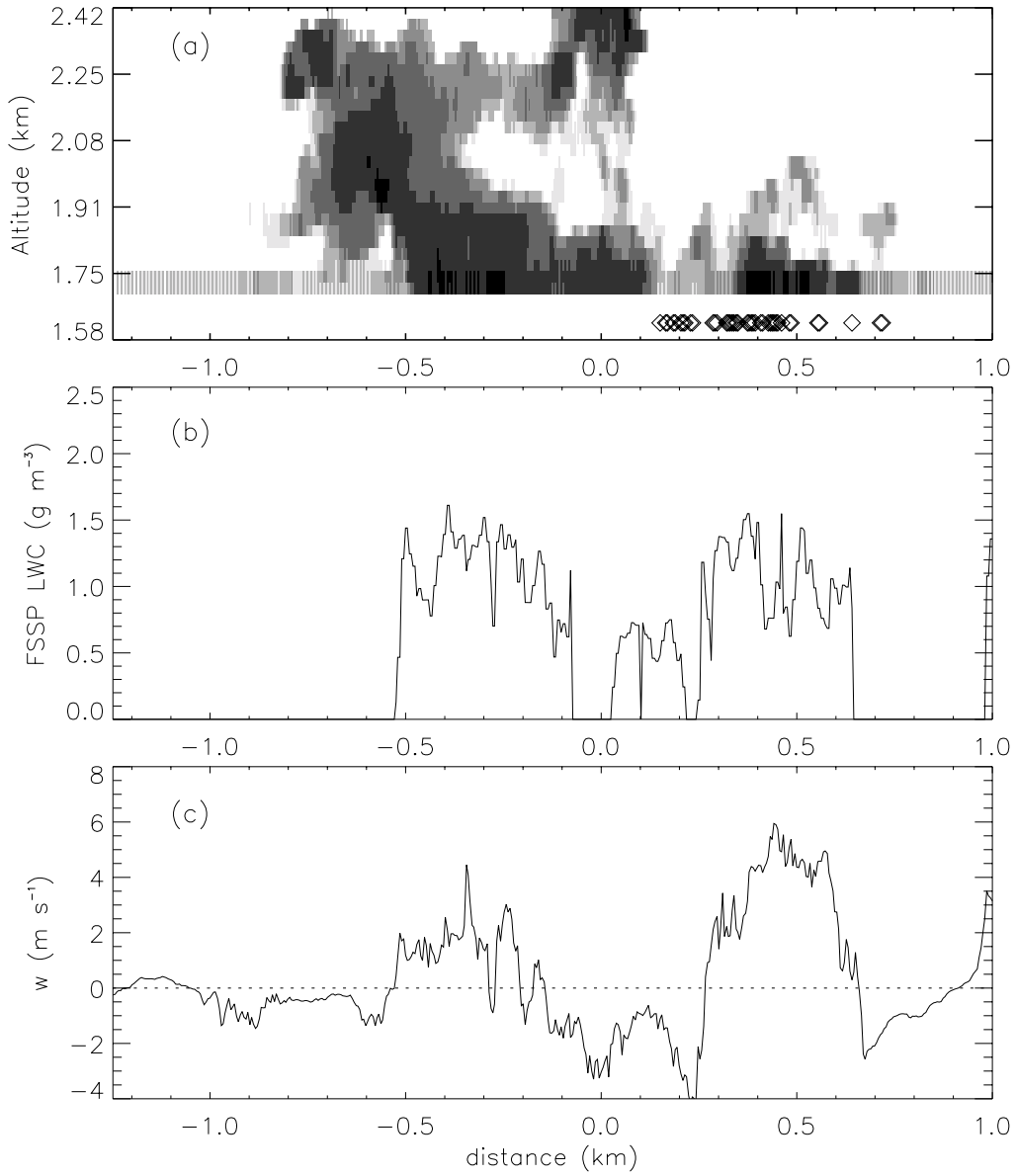

Fig. 12. As in Fig. 11 except for the third penetration at 700 m above cloud base in cloud C5 on 5 August.

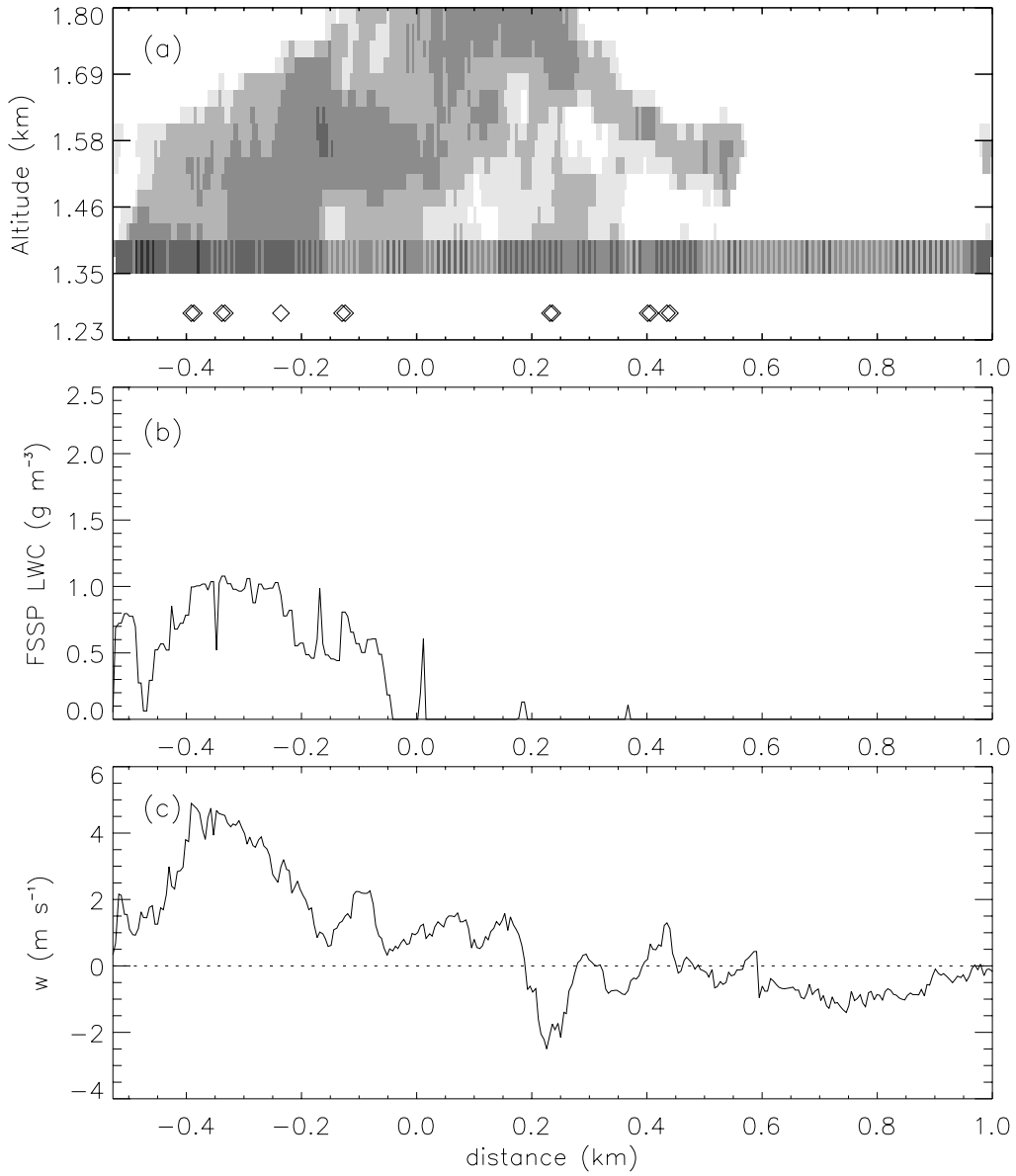

Fig. 13. As in Fig. 11 except for the fourth penetration at 380 m above cloud base in cloud C1 on 7 August.

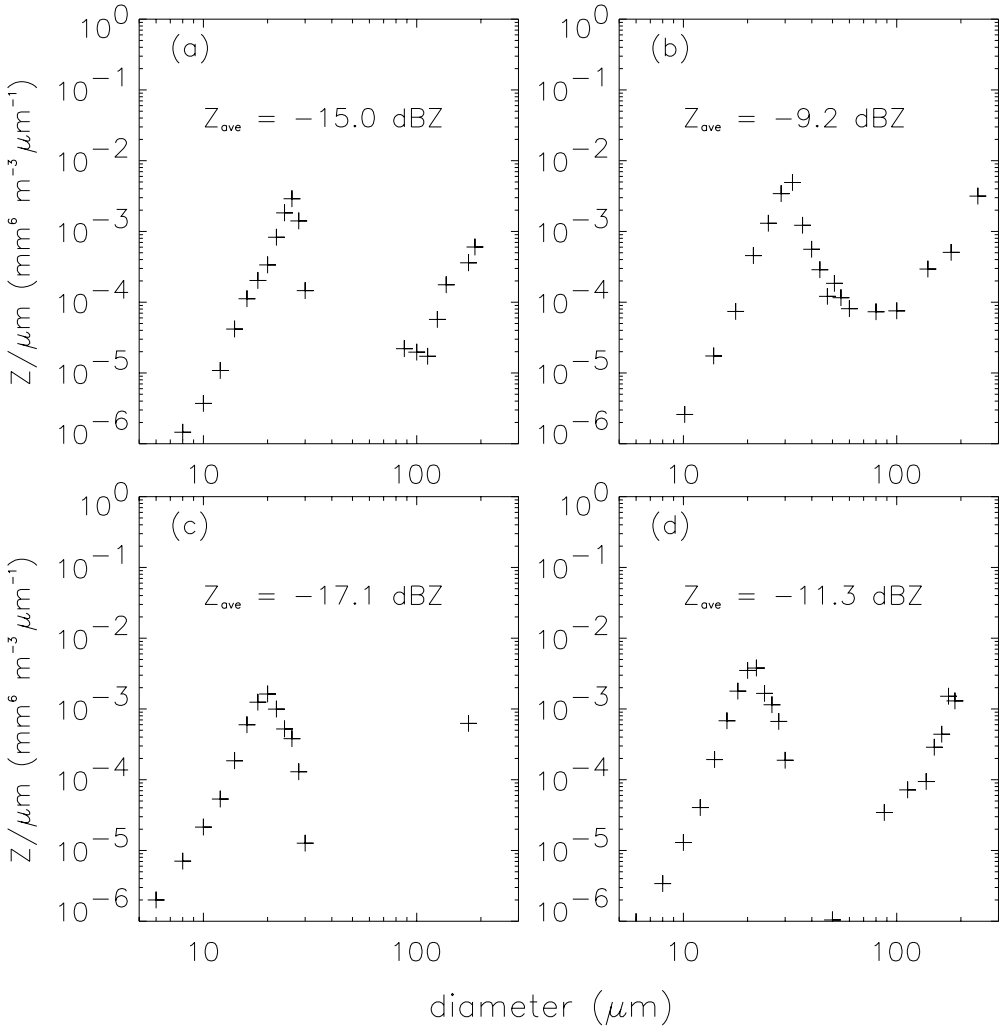

Fig. 14. As in Fig. 10, except the spectra have been weighted by reflectivity (D^6).

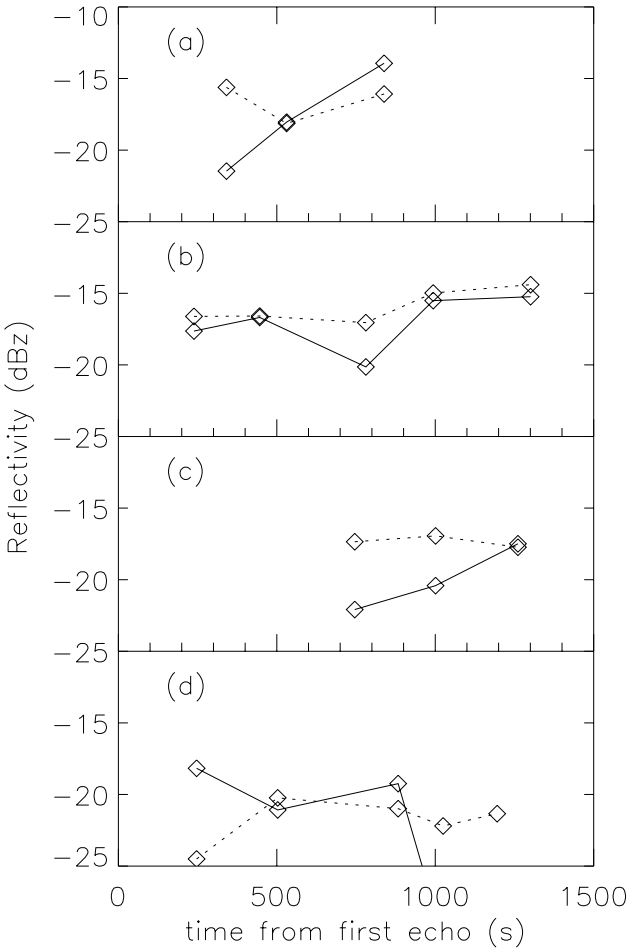

Fig. 15. Average calculated reflectivity for penetrations from clouds (a) C5, (b) C8, and (c) C9 on 5 Aug, and (d) C10 on 7 August. The dashed line represents the contribution from cloud droplets (Z_C) and the solid line represents the contribution from large droplets (Z_D). The zero time corresponds to the initial detection of the cloud as defined by a first echo of roughly -20 dBZ_e magnitude from measurements made by the CP-2 radar.

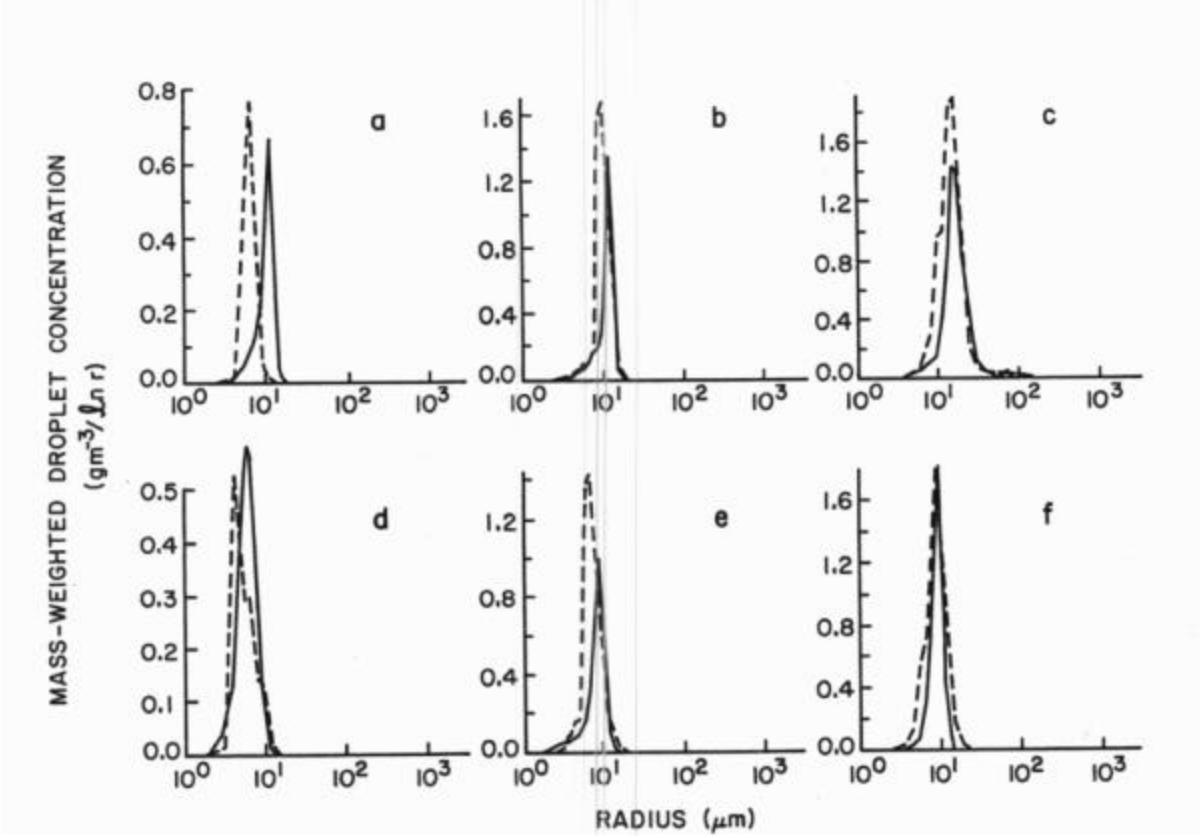

Fig. 16. Mass-weighted differential droplet spectra based on observations (solid line) and simulations (dotted line) using a parcel model including growth via condensation and stochastic coalescence. The top three are from Case 4 in Flossman *et. al.* (1985) for simulation times of (a) 200 s (200 m), (b) 600 s (760 m), and (c) 1400 s (2090 m), and observation levels on 5 August of (a) 250 m, (b) 700 m, and (c) 1700 m above cloud base. The bottom three are from Case 3 in Flossman *et. al.* for simulation times of (a) 200 s (200 m), (b) 600 s (760 m), and (c) 1000 s (1260 m), and observation levels on 7 August of (a) 300 m, (b) 700 m, and (c) 1100 m above cloud base.